



# RESEARCH MEMORANDUM

EXPERIMENTAL INVESTIGATION OF EJECTOR-NOZZLE  
METAL TEMPERATURES

By Thomas B. Shillito and William K. Koffel

Lewis Flight Propulsion Laboratory  
Cleveland, Ohio

NATIONAL ADVISORY COMMITTEE  
FOR AERONAUTICS  
WASHINGTON

February 27, 1957  
Declassified October 16, 1961

ПОЧЕМУ МЯ

СИДИ В КАРДИНАЛСКОМ

ВОДЫ СОЛНЦА И СОЛНЦА СОЛНЦА

ЗАЩИТАЮЩИЙ СВЯТОМ

БОГИ СОЛНЦА И СОЛНЦА СОЛНЦА

СОЛНЦА СОЛНЦА СОЛНЦА СОЛНЦА

NACA RM E56K20

## NATIONAL ADVISORY COMMITTEE FOR AERONAUTICS

RESEARCH MEMORANDUMEXPERIMENTAL INVESTIGATION OF EJECTOR-NOZZLE  
METAL TEMPERATURES

By Thomas B. Shillito and William K. Koffel

## SUMMARY

4245 A full-scale ejector installed on an afterburner was equipped with instrumentation to determine metal temperatures on both the primary-jet nozzle and the shroud. The afterburner was operated at exhaust-gas total temperatures up to 2990° F (3450° R), and the secondary airflow through the ejector was varied from 1.5 to 20 percent of the primary-gas flow out of the afterburner.

Low flow velocities in the secondary airstream gave low film heat-transfer coefficients compared with those for the primary-gas stream. Because of this, the primary-jet-nozzle metal temperature was closer to the primary-gas temperature than to the cooling-air (secondary-air) temperature. Critical primary-jet-nozzle metal temperatures were not reached, however, because of a favorable temperature distribution out of the afterburner. Even at a bulk afterburner-outlet temperature of 2990° F (3450° R), the effective gas temperature adjacent to the primary-jet-nozzle walls was only 350° F higher than the temperature of the turbine-discharge air. The low secondary-air heat-transfer coefficients also made the primary-jet-nozzle metal temperatures fairly insensitive to secondary airflow. For example, with an afterburner-outlet bulk temperature of 2990° F, the primary-jet-nozzle metal temperature decreased only 50° (from 1390° to 1340° F) as the secondary airflow increased from 1.5 to 20 percent of the primary-gas flow. Leakage of primary gas into the secondary-air passage caused local increases in primary-jet-nozzle metal temperatures of 250° F.

Mixing of the hot primary jet with the secondary flow controls the temperature of the shroud. Hence, maximum temperatures on the secondary shroud were much more sensitive to secondary airflow than were temperatures on the primary-jet nozzle. At secondary airflows less than 7 percent of the primary-gas flow, shroud temperatures exceeded primary-jet-nozzle temperatures.

## INTRODUCTION

Aircraft-engine ejector nozzles are generally used on engines equipped with afterburners. In such applications, the nozzle components must remain cool enough to ensure structural soundness at useful afterburner-outlet temperatures. Flow of the relatively cool secondary air (generally ram air) through the ejector helps to provide the protection required. The primary-jet nozzle of the ejector is cooled by the flow of secondary air over its outside surface, and the amount of cooling which the primary-jet nozzle requires will depend to a large extent upon the gas temperature distribution at the afterburner outlet. The gas temperature distribution is a function of the fuel-air distribution and the persistence of any cooling-air layer which might be introduced along the outer wall of the afterburner. Obviously, as afterburner output approaches the theoretical maximum, the primary-jet-nozzle metal temperatures will depend entirely upon cooling afforded by the secondary air-stream unless another source of cooling such as fuel can be utilized.

The ejector shroud is protected by the layer of secondary air which separates it and the primary-jet nozzle. It is exposed to severe heating only after this cool layer of air and the primary-gas stream have become mixed and the surface is exposed directly to relatively high-temperature air-gas mixtures.

Little is known about ejector design cooling requirements or of metal temperatures actually reached on operating ejector nozzles. In order to provide some insight into cooling and heating mechanisms involved in an ejector nozzle and to determine maximum temperatures and their locations, temperature instrumentation was installed on some of the components of a full-scale ejector during an engine and ejector performance investigation at the NACA Lewis laboratory.

The ejector was installed on an afterburner which was operated at bulk outlet temperatures up to  $2990^{\circ}$  F ( $3450^{\circ}$  R) in an altitude test chamber. Temperature measurements were obtained on components of the primary-jet nozzle and the shroud; and data were obtained at two afterburner-outlet temperatures, at two ejector diameter ratios, and for a range of over-all pressure ratios and secondary weight flows.

## APPARATUS

### Ejector Nozzle

Both the primary-jet nozzle and the shroud were of iris-type construction and were variable. The primary-jet nozzle had 24 leaves which were 0.06 inch thick. A drawing of one of the leaves is shown on figure 1. The leaves were of single-skin construction and each had two stiffeners on the downstream face which carried the actuator hinge points.

When the nozzle opens, pie-shaped openings form between adjacent leaves; and these openings are covered by the filler pieces shown on figure 1. The filler pieces, which were 0.06 inch thick, were loosely attached to the upstream surface of the primary leaves and were held against them by the pressure of the primary-gas flow.

The secondary shroud had 24 leaves of double-skin (0.04-in.) construction, as shown in figure 2. Each leaf had a stiffener on the inner surface. Filler pieces slide into pockets in the edges of the double-wall secondary leaves. Figure 3 is a photograph of the assembled shroud as viewed from the inside.

A schematic representation of the ejector nozzle (fig. 4) shows the relative positions of the primary-jet nozzle and the shroud. The shaded areas represent partial obstructions to the flow of secondary air caused by linkages, stiffeners, and so forth.

#### Installation

The ejector nozzle was installed on an afterburner-equipped turbojet engine which had a dry sea-level static-thrust rating of about 10,000 pounds. An exterior view of the afterburner-ejector assembly in the altitude test chamber, where the experiments were conducted, is shown in figure 5. Ejector secondary air was directed from an external source through a special line to an annular plenum chamber surrounding the afterburner near its upstream end. The secondary air passed from the plenum chamber to the ejector through an annular passage surrounding the afterburner. The secondary-air ducting and passage around the afterburner are shown schematically in figure 6.

The afterburner was 32 inches in diameter, and the length from the plane of fuel injection to the primary-nozzle hinge plane was 65 inches. Fuel was injected through 20 radial spray bars, each of which had orifices spraying from both sides of the bar normal to the airstream at 12 different radial positions. Details of the spray-bar hole distribution and their relation to the inner and outer walls of the afterburner flow passage are shown in figure 7.

A corrugated louvered liner extended from the fuel spray bars to a point just upstream of the primary-jet-nozzle hinge point. The mean flow-passage height of the louvered liner was  $5/8$  inch. Its downstream end was closed.

A two-ring annular V-gutter flameholder with gutter diameters of 11.04 and 25.52 inches was used. The flameholder was located at two alternate axial positions,  $9\frac{1}{2}$  and  $14\frac{1}{2}$  inches downstream of the fuel spray bars.

### Instrumentation

The primary-jet-nozzle gas flow was determined from measurements of total and static pressures and temperatures at the engine inlet, overboard bleed flow from the engine, and total fuel flow to the engine and afterburner. Secondary airflow was determined from measurements of total and static pressures and temperatures in the secondary-air supply line (fig. 6). Fuel flows to the engine and afterburner were measured with rotating vane-type flowmeters.

Total pressure at the inlet to the primary-jet nozzle was measured with a diametrical rake. The tubes in the rake were spaced to give readings in 19 equal areas. Total pressure and temperature of the secondary flow were measured at three radial positions at each of four positions  $90^\circ$  apart around the annular secondary-flow passage. These measurements at both the primary-jet-nozzle inlet and in the secondary-flow passage were at the same axial position as indicated in figure 4.

Temperature measurements on the inner surfaces of both the primary-jet nozzle and the shroud were taken at three circumferential locations spaced  $120^\circ$  apart which were designated  $0^\circ$ ,  $120^\circ$ , and  $240^\circ$  locations. Thermocouple locations on the leaves and filler pieces were the same for all three circumferential locations. The locations of the thermocouples on the primary-jet nozzle are shown in figure 1, and the thermocouples are designated according to location as a, b, c, and d. The thermocouples were chromel and alumel wire with magnesia insulation inside stainless-steel tubing which was swaged to 0.062-inch outside diameter. The ends of the thermocouples were brazed into holes in the metal skin with the thermocouple junction flush with the hot-gas side of the metal. The inset sketch in figure 1 shows a typical primary-jet-nozzle thermocouple installation.

Thermocouples on the shroud leaves were installed at the locations shown in figure 2. The thermocouples used were of the swaged type similar to those for the primary nozzle. The junctions of thermocouples a, b, c, and d, which can be seen in the photograph of figure 3, were welded to the inner surface and the thermocouple leads were laid along the surface. The leads for thermocouples e and f, which measured the metal temperature of the stiffener, were inside the stiffener and cannot be seen in figure 3.

### PROCEDURE

All the data were taken under steady-state operating conditions. For each series of runs, the engine and test-chamber conditions, the afterburner-outlet temperature, and the ejector geometry were fixed; and systematic variations in ejector secondary airflow were made. All runs were made with an ejector spacing ratio  $l/D_p$  of about 0.73.

The primary-gas total temperatures which are used in this report are bulk values and were calculated by well-known flow continuity methods which utilize primary-jet-nozzle mass flow, inlet pressure, and effective throat area.

The stems of the thermocouples on the primary-jet-nozzle leaves and filler pieces (fig. 1) were exposed to the flow of secondary air. A so-called "fin-effect" correction had to be made to account for local overcooling at the point of measurement. Local overcooling occurs because heat is conducted away from the point of measurement through the stems of the thermocouples and is then transferred by convection to the secondary air. The corrections were made according to the methods outlined in chapter 2 of reference 1.

## RESULTS AND DISCUSSION

### Primary-Jet-Nozzle Cooling

General characteristics. - At the conditions investigated, convective cooling of the primary-jet nozzle by the ejector secondary air was weak and did not materially affect temperatures of the components. Despite the absence of strong cooling, however, metal temperatures did not exceed or even approach critical values, apparently because of an afterburner-outlet temperature distribution that was favorable to the nozzle for cooling. This was true even at an afterburner-outlet temperature of  $2990^{\circ}$  F ( $3450^{\circ}$  R), where the highest metal temperatures on the primary-jet-nozzle leaves were about  $1400^{\circ}$  F, as shown in figure 8.

Figure 8, which shows primary-jet-nozzle leaf temperatures at the nozzle throat and secondary-air temperature as a function of the ratio of secondary-airflow to primary-gas flow, illustrates that convective cooling is not too significant. The metal temperature of the leaf changed only slightly (approx.  $50^{\circ}$  F) as the secondary airflow increased from 1.5 percent to 20.0 percent of the primary-gas flow. Furthermore, part of the trend of metal temperature with secondary airflow can be attributed to the change in secondary-air temperature shown in the lower part of the figure. The ejector secondary air was ducted from the annular plenum chamber (figs. 5 and 6) through the passage surrounding the afterburner and was heated by the afterburner walls. The temperature of the secondary air at the ejector inlet thus decreased with increasing secondary airflow.

Actual gas temperatures adjacent to the primary nozzle were not measured. Consideration of the convective heat-transfer process, however, clearly illustrates the existence of a relatively cool gas layer adjacent to the primary-jet-nozzle surface. The metal reaches some temperature between the temperatures of the gas and the cooling air and is dependent

upon the local film heat-transfer coefficients for the cooling air and the gas. In equation form,  $\frac{T_g - (T_m + 460)}{(T_m + 460) - T_a} = \frac{h_a}{h_g}$ . Estimates of heat-

transfer coefficients obtained from reference 2 showed that the ratio  $h_a/h_g$  was very low (because of the low flow velocities of the secondary air) and reached a value of only 0.18 when the secondary airflow was 20 percent of the primary-gas flow. It is obvious from the equation that the metal temperature  $T_m$  was much closer to the gas temperature than to the cooling-air temperature. The effective value of this gas temperature, therefore, had to be much lower than the primary-gas bulk temperature in order to give the observed metal temperatures which are shown on figure 8.

Graphic illustration of the existence and effectiveness of the cool gas layer is given in figure 9. Figure 9 shows a comparison of observed primary-jet leaf temperatures with values calculated for two gas temperatures,  $2990^{\circ}$  F ( $3450^{\circ}$  R), which corresponds to the observed bulk temperature, and  $1100^{\circ}$  F ( $1560^{\circ}$  R), which corresponds to the turbine-discharge temperature. The curve through the experimental data has been extrapolated to zero secondary airflow, and the intercept obtained on the temperature scale indicates that the gas temperature adjacent to the nozzle surface was only  $1450^{\circ}$  F ( $1910^{\circ}$  R), an increase over the turbine-discharge temperature of only  $350^{\circ}$  F. This indicates that the film of turbine-discharge gas emitted from the cooling-liner louvers must have persisted to a large extent through the exhaust nozzle. The liner cooling-gas discharge and the spray bars (fig. 7), which were designed to keep the outermost 10 percent of the air fuel free, apparently combined to provide the low level of temperature in the gas brushing the primary-jet-nozzle surface.

If higher temperatures existed at the wall of the nozzle, such as might be the case with increased values of afterburner output, a serious cooling problem might exist. This would demand higher secondary-air velocities over the primary nozzle than existed in the ejector investigated, possibly finning to increase the convective heat transfer, or even some form of film cooling.

In computing the curves shown on figure 9, equation (9-32c) of reference 2 (p. 242) was used. Skin temperatures at the downstream edge of the nozzle, where the highest heat flux would occur, were computed for sonic flow through the nozzle and for secondary-air temperatures corresponding to those shown in figure 8. The thermal resistance of the metal skin and radiation from the gases were neglected.

Effect of construction features and operating conditions. - A comparison of leaf and filler temperatures on figure 10 shows that the filler temperature was about  $250^{\circ}$  F hotter than the leaf temperature at

all secondary airflows. It appears from figure 8 that without any convective cooling the maximum temperature of any of the primary-jet-nozzle components would be about  $1450^{\circ}$  F. The  $250^{\circ}$  F difference noted in figure 10 must therefore be attributed to leakage which put hot gases on the outside of the filler pieces and reduced the effectiveness of the insulating layer of cool gas on the inside surface of the filler pieces. The apparent source of this leakage is shown in the photograph of figure 11. Cracks which existed between the primary-leaf hinges were not covered completely by the upstream ends of the filler pieces, particularly with the nozzle in the open or afterburning position. The gas leakage also caused the temperature on the upstream part of the filler piece to be slightly higher than the downstream temperature. This is shown by the top pair of curves in figure 12.

The lower pair of curves in figure 12 shows how overlapping of the leaves and the filler pieces allowed the edges of the leaves to be from  $50^{\circ}$  to  $90^{\circ}$  F cooler than the center portions of the leaves. The higher thermal resistance caused by the overlap provided a protective action for the leaf. By a similar token, the overlap might make the edge of the filler piece the critical zone for cooling with more severe afterburner-outlet temperature profiles.

A reduction in the primary-gas temperature from  $2990^{\circ}$  F ( $3450^{\circ}$  R) to  $2530^{\circ}$  F ( $2990^{\circ}$  R) reduced the primary-leaf temperature between  $350^{\circ}$  F and  $450^{\circ}$  F, as shown in figure 13. The curves in figure 13 show that the leaf temperatures at a primary-gas temperature of  $2530^{\circ}$  F ( $2990^{\circ}$  R) were more sensitive to secondary airflow rate than were the leaf temperatures at  $2990^{\circ}$  F ( $3450^{\circ}$  R), a result contrary to what could logically be expected. No reasons have been found for this apparently inverted behavior.

#### Ejector-Shroud Heating

General mechanism. - The ejector shroud does not have a forced-convection cooling system similar to that provided for the primary-jet nozzle. (During the investigation, the outside of the shroud was exposed to the relatively still, low-pressure air which ventilated the altitude test chamber.) Internally, the shroud has a blanket of secondary air which, until it becomes mixed with the hot primary gas, protects it and keeps its temperature low. Processes that are important in the mixing of gas streams can therefore be expected to control the temperatures reached by parts of the ejector shroud. In the mixing of two coaxial streams at the same temperature, the mixing boundaries are functions of the ratio of velocities in the streams (ref. 3). A similar influence of velocity ratio could be expected in the mixing processes occurring in an ejector.

A set of data selected to illustrate the connection between mixing of the gas streams and the shroud metal temperature is shown in figure 14. The upper part of the figure shows the ratio of primary-gas velocity to secondary-air velocity in the plane of the primary-jet-nozzle exit as a function of the ratio of secondary airflow to primary-gas flow. The velocity ratio decreases with increasing airflow ratio, as would be expected. Changes in flow conditions occur axially in an ejector so that the values shown are only indicative of conditions at the beginning of the mixing process.

The variation with airflow ratio of metal temperatures measured on the shroud at the furthest upstream thermocouple location is shown in the lower part of the figure. Secondary-air temperature is also shown for reference. At low airflow ratios (below 0.10), the mixing boundary is upstream of the shroud thermocouple location and the shroud metal temperature decreases rapidly with increasing airflow ratio, reflecting changes in the amount of mixing of the secondary air and the primary gas which occurs upstream of the thermocouple. At an airflow ratio of 0.10 an apparent discontinuous change in shroud temperature variation takes place. This discontinuity is believed to be the point at which the mixing boundary passes the thermocouple location. At airflow ratios greater than 0.10 the shroud wall at the point of measurement was in contact with secondary air that had not been heated by mixing with the primary gas. The shroud temperature was from 100° to 180° F higher than the secondary air, possibly as a result of radiation from the primary gases. Some convective cooling of the metal by the secondary air at airflow ratios above 0.10 is indicated by the decrease in temperature difference between the metal and the air as the airflow ratio increases.

Further evidence of this progressive mixing is the manner in which the temperature of the shroud leaves increases with distance downstream. A plot of typical data which shows how the metal temperature increases with distance along the shroud is shown in figure 15. Curves are shown for different ratios of ejector secondary airflow to primary-gas flow; on the abscissa scale the thermocouple positions are noted for reference. At a given airflow ratio, mixing of secondary airflow and primary-gas flow becomes more complete with distance downstream. The mixture of gas and air adjacent to the shroud surface thus becomes hotter with distance downstream, and the shroud surface temperature responds directly to the mixture temperature.

For the conditions shown on figure 15, the maximum shroud-leaf temperatures occur at the downstream edge of the shroud or thermocouple d location. In some cases thermocouple c gave a reading slightly higher than thermocouple d. This occurred at ejector diameter ratios of 1.29 and particularly at low over-all pressure ratios. It is believed that, when thermocouple c reading was higher than thermocouple d reading, there was a flow separation near the downstream edge of the shroud with

an attendant backflow of cool ambient air from the test chamber. In subsequent data plots, the higher reading of either thermocouple c or d is used to illustrate effects of different variables.

Effect of operating conditions on shroud skin temperature. - A change in the ejector diameter ratio (ratio of shroud-exit diam. to primary-jet-nozzle diam.) had a pronounced effect on the shroud metal temperature. Figure 16 shows that at a primary-gas total temperature of about  $2940^{\circ}$  F ( $3400^{\circ}$  R) and an over-all pressure ratio of 4.9, the shroud was from  $300^{\circ}$  to  $550^{\circ}$  F hotter at a diameter ratio of 1.1 than it was at a diameter ratio of 1.29. Among the factors that could cause this is the difference in initial velocity ratio. At a given secondary airflow, the initial ratio of primary-gas velocity to secondary-air velocity is higher for the lower diameter ratio because of higher secondary-air pressures. This would give a higher mixing rate for the lower diameter ratio.

A comparison of temperatures on the secondary shroud and the primary-jet nozzle shows that for this particular ejector geometry the shroud could be the critical component. The shroud temperature at an airflow ratio of 0.05 and a diameter ratio of 1.1 is about  $1500^{\circ}$  F (fig. 16). This is about  $100^{\circ}$  F hotter than the temperature of the primary-jet-nozzle leaf (fig. 8) and only  $150^{\circ}$  F less than the filler-piece temperature (fig. 10). In the absence of gas leakage, which would cause the filler-piece temperature to be artificially high, the shroud is hotter than the primary nozzle at all airflow ratios below about 0.07.

The response of the ejector-shroud temperature to changes in primary-gas bulk temperature was about the same as for the primary-jet nozzle. Figure 17 shows that a  $400^{\circ}$  R increase in primary-gas bulk temperature increased the shroud leaf temperature from  $400^{\circ}$  to  $500^{\circ}$  F.

The influence of over-all pressure ratio on the shroud metal temperature was highly dependent upon both the level of pressure ratio and the diameter ratio. As figure 18(a) shows, an increase in pressure ratio from about 4.8 to about 6.2 caused only a slight decrease in shroud metal temperature for a 1.29-diameter-ratio ejector. The absence of any appreciable change in temperature with pressure ratio results from the fact that at these pressure ratios internal choking prevents the established pattern of internal flow from being affected by changes in over-all pressure ratio. However, a very marked change is noted as the over-all pressure ratio is lowered to a value near 2.0. The metal temperature decreases sharply at the low secondary airflows. At an ejector diameter ratio of 1.10 (fig. 18(b)), the effect of reducing the over-all pressure ratio to about 2.0 is much less pronounced than for the higher-diameter-ratio ejector.

### Tabulated Data

The performance curves presented in this report were plotted from data contained in tables I to III. Table I gives general information as to engine, afterburner, ejector, and test-chamber operating conditions and describes the significant ejector geometrical ratios. Temperatures measured on the primary-jet-nozzle components are given in table II (corrected for fin effect) and on the ejector shroud, in table III. Some thermocouples malfunctioned during the course of testing, and readings which were obviously in error have thus been deleted. Inspection of the values reveals that temperatures in the  $120^{\circ}$  location of the primary-jet nozzle (table II) appear abnormally low and thus questionable.

### CONCLUDING REMARKS

Metal temperatures were determined on both the primary nozzle and the shroud of an ejector installed on an afterburner having exhaust-gas temperatures as high as  $2990^{\circ}$  F ( $3450^{\circ}$  R). In the ejector investigated, convective cooling of the primary-jet nozzle was weak because of low secondary-air velocities over its surface. Strong cooling was not too essential, however, because of an afterburner-outlet profile that was favorable for cooling. This fact demonstrates that close attention to and control of the afterburner-outlet profile, by means of both the control of fuel distribution and the use of afterburner wall liners, is probably one of the most effective ways of ensuring satisfactory metal temperatures in the primary-jet nozzle. Higher afterburner-outlet bulk temperatures will, however, complicate the problem by leading to less favorable temperature profiles. If convective cooling is depended upon, higher secondary-air velocities over the primary-jet nozzle and use of techniques such as finning will be required. In extreme cases, convective cooling by the secondary air might be incapable of providing metal temperatures low enough to ensure structural soundness; and film cooling in some form might be required.

Leakage of hot gas into the secondary-flow passage through openings in the iris components of the primary-jet nozzle could create problems. Such leaks in the ejector investigated increased local metal temperatures by  $250^{\circ}$  F.

Rapid mixing of the primary jet with the secondary airflow prevents the shroud from benefiting as much as the primary-jet nozzle from a favorable afterburner-outlet temperature profile. As a result, the ejector shroud appears to be potentially more critical than the primary-jet nozzle. The metal temperature of the shroud, which was very sensitive

to secondary-flow rate, exceeded primary-jet-nozzle temperatures ( $1400^{\circ}$  F) in one case when the secondary airflow was less than 7 percent of the primary-gas flow.

Lewis Flight Propulsion Laboratory  
National Advisory Committee for Aeronautics  
Cleveland, Ohio, November 21, 1956

## APPENDIX - SYMBOLS

$D_p$	primary-jet-nozzle throat diameter, ft
$D_s$	shroud-outlet diameter, ft
$h_a$	cooling-air-film heat-transfer coefficient, Btu/(sec)(sq ft)(°F)
$h_g$	primary-gas heat-transfer coefficient, Btu/(sec)(sq ft)(°F)
$l$	distance between primary-jet-nozzle outlet and shroud outlet, ft
$P_p$	primary-jet-nozzle total pressure, lb/sq ft abs
$P_s$	secondary-air total pressure, lb/sq ft abs
$P_1$	engine-inlet total pressure, lb/sq ft abs
$P_5$	turbine-outlet total pressure, lb/sq ft abs
$p_0$	exhaust static pressure, lb/sq ft abs
$T_{a,3}$	cooling-air (secondary-air) temperature at ejector entrance, °R
$T_g$	primary-gas (or afterburner-outlet) bulk total temperature, °R
$T_{g,p}$	primary-gas temperature adjacent to primary-jet-nozzle surface, °R
$T_m$	metal temperature, °F
$T_{s,3}$	secondary-air total temperature at ejector entrance, °R
$T_1$	engine-inlet total temperature (or initial secondary-air temperature at plenum-chamber inlet), °R
$T_5$	turbine-outlet total temperature, °R
$w_{a,1}$	engine-inlet airflow, lb/sec
$w_{f,ab}$	afterburner fuel flow, lb/hr
$w_{f,e}$	engine fuel flow, lb/hr
$w_p$	primary-jet-nozzle (or afterburner-outlet) gas flow, lb/sec
$w_s$	secondary airflow, lb/sec

4245

## REFERENCES

1. Boelter, L. M. K., Cherry, V. H., Johnson, H. A., and Martinelli, R. C.: Heat Transfer Notes. Univ. Calif. Press (Berkley), 1948.
2. McAdams, William H.: Heat Transmission. Third ed., McGraw-Hill Book Co., Inc., 1954.
3. Forstall, Walton, Jr., and Shapiro, Ascher H.: Momentum and Mass Transfer in Coaxial Gas Jets. Meteor Rep. No. 39, Dept. Mech. Eng., M.I.T., July 1949. (Bur. Ord. Contract NOrd 9661.)

TABLE I. - OPERATING CONDITIONS

Run	Exhaust static pressure, $p_0$ , lb sq ft abs	Engine- inlet total pressure, $P_1$ , lb sq ft abs	Engine- inlet total temper- ature, $T_1$ , °R	Engine- inlet airflow, $w_{a,1}$ , lb/sec	Engine fuel flow, $w_f, e$ , lb/hr	Turbine- outlet total tempera- ture, $T_5$ , °R	Turbine- outlet total pressure, $P_5$ , lb sq ft abs	After- burner fuel flow, $w_{f, ab}$ , lb/hr	Ejector primary- gas total temper- ature, $T_g$ , °R	Ejector primary- gas total pressure, $P_p$ , lb sq ft abs
1	517	1152	494	93.55	4870	1569	2828	11,840	3415	2500
2	526	1156	494	93.75	4850	1565	2824	11,800	3384	2496
3	519	1152	494	93.46	4850	1564	2820	11,760	3395	2491
4	520	1155	493	93.77	4890	1564	2842	12,020	3442	2519
5	497	1158	493	93.94	4860	1564	2832	11,990	3399	2509
6	490	1159	494	93.97	4860	1562	2830	11,930	3398	2510
7	1077	1157	495	93.54	4890	1555	2837	11,630	3445	2518
8	1091	1151	495	93.32	4865	1552	2824	11,670	3433	2506
9	1113	1150	494	93.27	4875	1549	2829	11,870	3436	2509
10	1101	1154	494	93.69	4900	1555	2842	12,100	3435	2519
11	1100	1156	494	93.65	4930	1559	2854	12,350	3462	2530
12	1108	1157	494	93.91	4910	1550	2848	12,100	3436	2524
13	520	1154	493	93.71	4840	1557	2821	11,750	3391	2409
14	536	1154	493	93.83	4935	1563	2859	12,260	3454	2530
15	544	1153	493	93.83	4935	1561	2857	12,310	3450	2529
16	512	1160	493	94.13	4940	1565	2863	12,330	3449	2535
17	509	1155	493	93.75	4930	1563	2857	12,330	3462	2530
18	510	1155	494	94.12	4935	1563	2857	12,290	3435	2530
19	502	1159	493	94.28	4915	1559	2854	12,190	3416	2527
20	1104	1157	494	93.89	4920	1552	2852	12,100	3428	2523
21	1115	1156	494	93.80	4935	1558	2858	12,120	3448	2527
22	1120	1158	494	94.02	4950	1550	2863	12,120	3439	2532
23	1098	1152	494	93.40	4925	1556	2850	12,120	3453	2520
24	1089	1144	494	92.99	4910	1559	2840	12,070	3467	2513
25	1100	1153	494	93.52	4910	1554	2844	12,070	3445	2518
26	1099	1146	493	93.07	4875	1550	2828	12,050	3450	2507
27	1076	1143	493	92.80	4880	1553	2827	12,260	3450	2504
28	427	1140	507	91.53	4720	1549	2754	11,395	3361	2428
29	406	1161	508	91.45	4740	1544	2760	11,340	3387	2434
30	398	1164	508	91.36	4755	1551	2767	11,340	3439	2446
31	392	1160	507	91.29	4760	1554	2769	11,375	3439	2444
32	381	1163	506	91.78	4735	1548	2761	11,395	3387	2439
33	369	1168	505	92.22	4740	1546	2772	11,500	3376	2448
34	364	1168	505	92.19	4740	1542	2772	11,500	3394	2454
35	354	1150	520	88.33	4360	1531	2679	11,620	3371	2387
36	595	1151	523	88.22	4340	1532	2677	11,450	3372	2385
37	983	1150	523	88.05	4350	1532	2682	11,450	3403	2393
38	465	1154	523	88.50	4370	1536	2693	9,110	2967	2456
39	469	1157	523	88.52	4450	1551	2731	9,400	3033	2487
40	477	1158	523	88.76	4350	1531	2682	8,910	2943	2450
41	470	1159	523	88.68	4395	1537	2716	9,155	2990	2470
42	472	1156	524	88.56	4395	1538	2709	9,110	2993	2467
43	473	1162	524	88.60	4380	1538	2701	9,155	2971	2460
44	449	1168	526	89.18	4395	1540	2710	9,055	2962	2470
45	462	1166	526	89.18	4450	1543	2737	9,205	2995	2487
46	465	1163	526	89.24	4445	1539	2736	9,170	2998	2489
47	465	1165	526	89.18	4420	1533	2738	9,155	3002	2489
48	478	1164	526	89.15	4410	1530	2728	9,095	2992	2484
49	475	1164	523	89.18	4410	1527	2728	9,095	2992	2485
50	460	1170	522	89.52	4410	1545	2722	9,055	2955	2477
51	479	1161	522	89.06	4395	1543	2713	9,035	2964	2468
52	465	1176	522	89.70	4410	1543	2713	9,005	2925	2469
53	239	1132	523	86.91	4370	1553	2674	9,005	3016	2432
54	240	1140	523	87.36	4350	1552	2676	8,910	2990	2432
55	253	1138	523	87.31	4340	1551	2670	8,895	2979	2426
56	255	1137	523	87.40	4305	1549	2654	8,880	2945	2417
57	248	1137	523	87.28	4305	1551	2655	8,805	2960	2417

## AND EJECTOR CONFIGURATIONS

Ejector secondary-air total temperature, $T_{s,3}$ , °R	Ejector secondary-air total pressure, $P_{s,3}$ , lb sq ft abs	Ejector secondary airflow, $w_s$ , lb/sec	Corrected mass flow ratio, $\frac{w_s}{w_p} \sqrt{\frac{T_{s,3}}{T_g}}$	Diameter of primary-jet-nozzle throat, $D_p$ , in.	Ejector diameter ratio, $D_s/D_p$	Ejector spacing ratio, $l/D_p$	Over-all pressure ratio, $P_p/P_0$	Ejector total-pressure ratio, $P_{s,3}/P_p$	Air-flow ratio, $w_s/w_p$	Run
540	1172	20.07	0.0830	28.46	1.103	0.7256	4.836	0.4688	0.2087	1
549	1055	16.35	.0683	28.46	1.103	.7259	4.746	.4227	.1697	2
560	979	12.86	.0544	28.46	1.103	.7259	4.798	.3930	.1339	3
575	919	9.66	.0410	28.46	1.103	.7252	4.845	.3648	.1002	4
601	850	7.04	.0307	28.45	1.103	.7255	5.048	.3388	.0729	5
637	794	4.98	.0223	28.44	1.104	.7257	5.123	.3163	.0516	6
538	1350	20.33	.0836	28.43	1.104	.7263	2.338	.5361	.2116	7
542	1288	17.49	.0725	28.44	1.104	.7261	2.297	.5740	.1824	8
560	1207	13.55	.0570	28.44	1.104	.7261	2.254	.4811	.1413	9
590	1098	8.57	.0368	28.44	1.104	.7257	2.288	.4359	.0889	10
624	1025	4.91	.0216	28.44	1.104	.7257	2.300	.4051	.0509	11
647	977	2.64	.0118	28.45	1.103	.7255	2.278	.3871	.0273	12
542	810	18.62	.0773	28.44	1.293	.7264	4.805	.3241	.1934	13
540	786	16.91	.0692	28.44	1.293	.7264	4.719	.3107	.1751	14
550	734	13.78	.0570	28.45	1.292	.7262	4.649	.2902	.1427	15
559	666	10.20	.0424	28.45	1.292	.7262	4.950	.2627	.1053	16
588	604	6.92	.0295	28.45	1.292	.7262	4.970	.2387	.0717	17
623	566	4.60	.0202	28.45	1.292	.7262	4.960	.2237	.0475	18
673	529	2.97	.0136	28.44	1.293	.7264	5.033	.2093	.0306	19
540	1176	19.96	.0820	28.44	1.293	.7268	2.285	.4661	.2066	20
545	1160	16.61	.0684	28.44	1.293	.7268	2.267	.4590	.1721	21
557	1143	13.37	.0556	28.44	1.293	.7264	2.281	.4514	.1382	22
582	1098	9.46	.0404	28.44	1.293	.7264	2.295	.4357	.0984	23
600	1070	6.97	.0303	28.44	1.293	.7264	2.308	.4258	.0728	24
633	1060	4.62	.0206	28.44	1.293	.7264	2.289	.4210	.0480	25
673	1046	2.55	.0117	28.45	1.290	.7262	2.281	.4172	.0266	26
700	1010	1.38	.0072	28.45	1.291	.7262	2.327	.4034	.0144	27
553	793	19.84	.0856	28.45	1.292	.7272	5.685	.3266	.2110	28
559	708	15.76	.0682	28.45	1.292	.7276	5.995	.2909	.1678	29
568	646	13.24	.0573	28.48	1.291	.7268	6.146	.2641	.1411	30
592	579	9.63	.0426	28.48	1.291	.7268	6.234	.2369	.1027	31
603	524	6.97	.0312	28.47	1.291	.7271	6.402	.2148	.0740	32
646	480	4.66	.0215	28.47	1.291	.7267	6.636	.1961	.0492	33
707	433	2.64	.0127	28.47	1.291	.7267	6.743	.1764	.0279	34
743	476	2.93	.0151	28.45	1.284	.7255	6.743	.1994	.0322	35
735	518	2.83	.0146	28.45	1.278	.7258	4.008	.2172	.0312	36
719	905	2.92	.0148	28.45	1.279	.7258	2.434	.3782	.0322	37
731	463	2.74	.0150	27.04	1.286	.7245	5.282	.1885	.0303	38
688	502	4.06	.0214	27.04	1.287	.7245	5.302	.2018	.0449	39
664	528	5.35	.0281	27.04	1.287	.7234	5.136	.2155	.0591	40
630	570	7.49	.0380	27.04	1.288	.7234	5.254	.2131	.0827	41
605	629	10.32	.0513	27.04	1.288	.7245	5.227	.2550	.1141	42
592	703	14.50	.0715	27.04	1.288	.7245	5.200	.2858	.1602	43
597	1004	14.42	.0711	27.04	1.097	.7237	5.500	.4065	.1584	44
611	858	11.23	.0557	27.04	1.097	.7237	5.382	.3450	.1233	45
630	815	8.77	.0441	27.04	1.097	.7237	5.353	.3274	.0962	46
673	732	5.38	.0280	27.04	1.097	.7237	5.353	.2941	.0591	47
684	704	4.05	.0228	27.04	1.097	.7237	5.197	.2834	.0445	48
693	645	4.05	.0214	27.04	1.144	.7282	5.232	.2596	.0445	49
688	590	3.90	.0206	27.04	1.204	.7308	5.385	.2382	.0427	50
695	544	3.85	.0208	27.04	1.252	.7322	5.151	.2204	.0423	51
693	570	3.85	.0208	27.04	1.207	.7311	5.310	.2309	.0421	52
588	728	15.81	.0786	27.04	1.288	.7245	10.17	.2993	.1780	53
597	691	13.99	.0701	27.04	1.288	.7245	10.13	.2184	.1568	54
610	639	10.84	.0550	27.04	1.288	.7245	9.587	.2634	.1216	55
674	524	5.50	.0295	27.04	1.288	.7245	9.478	.2168	.0616	56
754	454	2.44	.0138	27.04	1.288	.7245	9.746	.1878	.0274	57

TABLE II. - METAL TEMPERATURES ON PRIMARY JET NOZZLE

Run	Circumferential location, deg											
	0				120				240			
	Filler	Leaf	Filler	Leaf	Filler	Leaf	Filler	Leaf	Filler	Leaf	Filler	Leaf
	Thermocouple											
	a	b	c	d	a	b	c	d	a	b	c	d
	Metal temperature, °F											
1	1528	----	1268	1342	1008	950	1024	----	1575	1528	1284	----
2	1610	----	1283	1351	1009	966	1030	----	1599	1542	1215	----
3	1593	----	1297	1354	1029	986	1050	----	1587	1536	1213	----
4	1656	----	1311	1373	1048	1027	1085	----	1539	1492	1211	----
5	1646	----	1319	1382	1068	1078	1099	----	1563	1532	1204	----
6	1643	----	1322	1390	1123	1150	1139	----	1566	1545	1233	----
7	1621	----	1279	1331	1002	943	1030	----	1570	1518	1179	----
8	1637	----	1275	1332	1021	962	1027	----	1565	1514	1180	----
9	1666	----	1298	1361	1046	988	1046	----	1579	1527	1188	----
10	1676	----	1318	1381	1067	1030	1072	----	1588	1541	1203	----
11	1669	----	1332	1394	1070	1091	1097	----	1612	1566	1243	----
12	1633	----	1313	1386	1091	1117	1101	----	1576	1535	1220	----
13	1598	----	1255	1344	974	920	1017	----	1567	1536	1161	----
14	1631	----	1299	1383	999	956	1026	----	1621	1585	1195	----
15	1646	----	1325	1397	1036	993	1047	----	1620	1589	1220	----
16	1675	----	1354	1416	1055	1039	1070	----	1628	1607	1244	----
17	1661	----	1355	1417	1056	1067	1093	----	1619	1609	1256	----
18	1673	----	1361	1419	1090	1122	1127	----	1621	1611	1268	----
19	1667	----	1378	1424	1129	1171	1160	----	1590	1579	1254	----
20	1571	----	1211	1299	936	878	967	----	1540	1479	1129	----
21	1610	----	1268	1335	993	955	1014	----	1584	1532	1205	----
22	1634	----	1287	1350	1014	982	1025	----	1583	1537	1209	----
23	1647	----	1300	1362	1037	1011	1048	----	1575	1539	1216	----
24	1651	----	1303	1360	1020	1036	1051	----	1573	1537	1220	----
25	1652	----	1305	1362	1053	1085	1069	----	1554	1518	1221	----
26	1638	----	1287	1354	1085	1143	1075	----	1571	1525	1235	----
27	1620	----	1339	1390	1118	1154	1102	----	1585	1549	1262	----
28	1422	----	1304	867	830	978	----	1489	1469	1051	----	
29	1501	----	1361	950	917	1046	----	1542	1532	1120	----	
30	1516	----	1387	967	1012	1062	----	1553	1548	1136	----	
31	1514	----	1395	996	1052	1065	----	1566	1555	1165	----	
32	1511	----	1392	1004	1112	1083	----	1548	1537	1168	----	
33	1523	----	1414	1049	1174	1143	----	1560	1539	1185	----	
34	1438	----	1433	1096	1205	1205	----	1541	1515	1195	----	
35	1482	----	1098	1140	1601	1254	----	1192	----	1124	----	
36	1466	----	1083	1124	1580	1233	----	1166	----	1098	----	
37	1456	----	1057	1114	1575	1208	----	1135	----	1052	----	
38	1362	----	1082	1082	1393	1155	----	1113	----	1082	----	
39	1423	----	1084	1078	1449	1183	----	1094	----	1063	----	
40	1356	----	1052	1021	1366	1100	----	1037	----	1021	----	
41	1384	----	1028	1002	1400	1102	----	1017	----	1012	----	
42	1366	----	1004	961	1402	1094	----	982	----	1009	----	
43	1333	----	960	895	1401	1077	----	933	----	1002	----	
44	1291	----	922	878	1385	1045	----	932	----	991	----	
45	1337	----	952	920	1383	1058	----	1000	----	924	----	
46	1336	----	962	941	1372	1057	----	1037	----	1047	----	
47	1346	----	1021	999	1361	1163	----	1131	----	1189	----	
48	1366	----	1037	1026	1355	1079	----	1173	----	1277	----	
49	1366	----	1037	1026	1340	1073	----	1121	----	1126	----	
50	1364	----	1057	1031	1333	1083	----	1120	----	1099	----	
51	1364	----	1025	1332	----	1088	----	1072	----	1046	----	
52	1364	----	1056	1025	1322	1067	----	1098	----	1109	----	
53	1331	----	918	859	1389	1063	----	940	----	994	----	
54	1338	----	927	873	1374	1055	----	964	----	1007	----	
55	1357	----	963	904	1357	1064	----	988	----	1010	----	
56	1367	----	1032	990	1346	1074	----	1085	----	1079	----	
57	1381	----	1080	1060	1339	1112	----	1148	----	1142	----	

TABLE III. - EJECTOR-SHROUD METAL TEMPERATURES

Run	Circumferential location, deg																	
	0						120						240					
	Thermocouple																	
	a	b	c	d	e	f	a	b	c	d	e	f	a	b	c	d	e	f
Temperature, °F																		
1	195	215	310	480	365	370	205	285	590	765	400	630	225	165	355	495	350	370
2	230	260	500	695	400	505	250	450	765	935	450	785	265	210	540	680	405	500
3	520	735	1000	1170	510	935	660	560	660	1115	545	955	440	330	780	915	480	685
4	680	750	1000	1170	630	975	755	860	1130	1270	660	1090	805	470	1050	1175	670	950
5	925	980	1230	1370	835	1215	950	1075	1315	1425	845	1260	995	605	1255	1355	925	1150
6	1125	1200	1420	1450	1065	1420	1095	1240	1455	1520	1065	1395	1180	730	1400	1520	1090	1350
7	190	210	325	370	370	410	185	265	600	750	405	620	195	160	425	555	350	395
8	215	235	405	440	395	460	210	340	695	845	430	685	220	180	505	645	380	455
9	315	425	640	635	455	630	390	635	865	1025	510	815	350	295	715	860	475	645
10	470	705	925	925	580	905	415	825	1035	1180	625	985	560	410	960	1080	655	895
11	475	770	1165	1135	780	1155	490	995	1260	1380	785	1195	445	505	1200	1285	905	1140
12	550	825	1280	1215	895	1275	525	1110	1400	1505	975	1345	500	585	1340	1395	1025	1285
13	170	195	240	210	245	265	165	200	330	475	395	440	170	150	325	410	345	355
14	190	210	275	250	270	305	180	245	435	590	525	525	185	155	375	460	365	390
15	215	245	355	300	305	380	210	305	585	750	690	665	225	175	500	605	445	505
16	180	330	545	440	420	555	300	485	820	965	905	885	295	250	735	870	565	715
17	450	535	830	690	615	820	465	715	1040	1150	1075	1070	560	410	975	1145	735	965
18	660	815	1095	970	865	1100	690	940	1225	1300	1250	1210	805	570	1170	1350	890	1160
19	870	1035	1270	1185	1060	1300	855	1145	1370	1420	1370	1330	1080	710	1310	1505	1070	1310
20	200	260	365	320	300	355	175	275	370	350	340	370	210	180	340	345	315	360
21	210	280	405	355	340	400	185	310	415	375	375	415	225	205	390	350	350	420
22	245	345	420	385	410	450	200	345	465	395	415	460	255	235	420	355	425	470
23	270	360	435	385	540	470	235	405	525	420	490	555	270	255	530	420	525	570
24	310	410	480	430	620	520	255	445	590	475	550	635	290	275	595	450	620	635
25	315	420	510	430	665	535	285	485	655	535	640	705	350	320	545	435	690	620
26	360	450	525	460	725	575	355	500	785	685	745	830	375	345	685	485	775	745
27	380	455	535	455	775	590	415	535	860	755	840	920	440	400	745	540	865	815
28	170	185	220	205	230	260	145	195	325	410	355	350	170	145	310	420	315	330
29	205	225	270	265	270	325	175	260	435	550	535	480	200	170	395	495	385	410
30	255	270	330	300	320	390	230	370	580	690	695	615	230	185	450	555	410	425
31	375	390	530	445	485	570	360	560	785	900	965	845	285	235	655	775	520	625
32	510	560	590	650	740	805	570	730	955	1060	1175	995	370	305	835	955	710	815
33	720	810	890	915	1010	1065	835	970	1165	1245	1350	1170	610	465	1075	1210	1010	1065
34	990	1100	1200	1185	1290	1300	1065	1255	1060	1430	1505	1350	1030	730	1310	1470	1295	1315
35	-----	1150	1130	-----	1215	-----	-----	685	1315	1445	1220	1315	730	-----	850	1245	1240	-----
36	-----	900	925	-----	1050	-----	535	1185	1300	1000	1190	400	-----	720	1135	1090	-----	-----
37	-----	580	535	-----	630	-----	330	610	425	795	670	310	-----	480	550	765	-----	-----
38	-----	1070	1060	-----	1070	-----	535	1150	1225	835	1085	630	-----	705	1100	795	-----	-----
39	-----	905	930	-----	955	-----	460	1060	1140	680	985	550	-----	650	1015	670	-----	-----
40	-----	755	765	-----	795	-----	370	880	970	545	805	430	-----	580	915	585	-----	-----
41	-----	520	545	-----	600	-----	260	685	790	470	610	320	-----	480	780	525	-----	-----
42	-----	295	345	-----	405	-----	210	460	570	385	410	245	-----	340	600	430	-----	-----
43	-----	205	235	-----	280	-----	185	300	395	320	305	205	-----	235	380	355	-----	-----
44	-----	270	310	-----	310	-----	165	275	420	305	280	560	-----	660	1065	605	-----	-----
45	-----	430	470	-----	460	-----	405	630	350	340	740	-----	810	1235	855	-----	-----	-----
46	-----	670	690	-----	660	-----	250	595	835	415	485	830	-----	900	1345	1060	-----	-----
47	-----	979	995	-----	960	-----	480	975	1130	645	895	975	-----	990	1435	1225	-----	-----
48	-----	1170	1170	-----	1130	-----	595	1140	1280	920	1070	1110	-----	1050	1450	1280	-----	-----
49	-----	1010	1020	-----	990	-----	550	1130	1240	895	1060	920	-----	1040	1350	1170	-----	-----
50	-----	875	900	-----	890	-----	580	1160	1260	890	1100	850	-----	1000	1285	1060	-----	-----
51	-----	755	770	-----	785	-----	560	1145	1240	825	1080	760	-----	900	1175	890	-----	-----
52	-----	770	790	-----	780	-----	585	1170	1265	905	1110	865	-----	1000	1305	1080	-----	-----
53	-----	170	190	-----	220	-----	155	290	400	315	275	235	-----	435	695	430	-----	-----
54	-----	180	200	-----	235	-----	165	350	485	335	310	270	-----	520	800	480	-----	-----
55	-----	225	250	-----	280	-----	200	490	620	365	410	360	-----	650	925	565	-----	-----
56	-----	420	465	-----	520	-----	470	990	1095	635	920	780	-----	900	1180	915	-----	-----
57	-----	810	830	-----	870	-----	670	1235	1335	930	1085	935	-----	1020	1305	1080	-----	-----

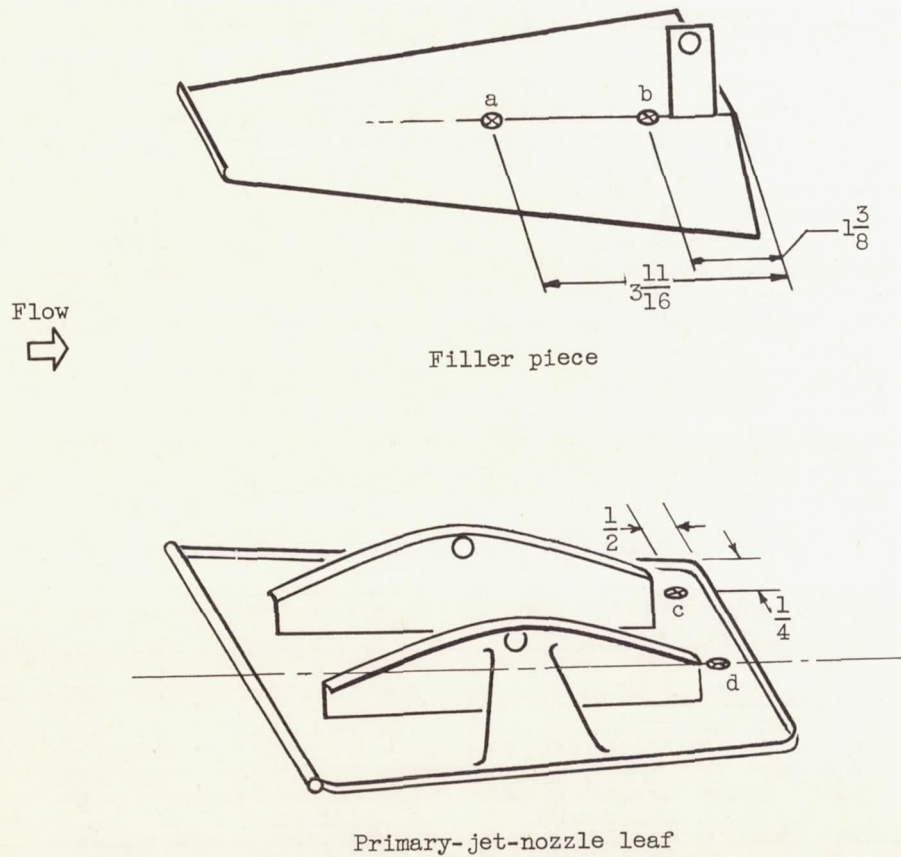
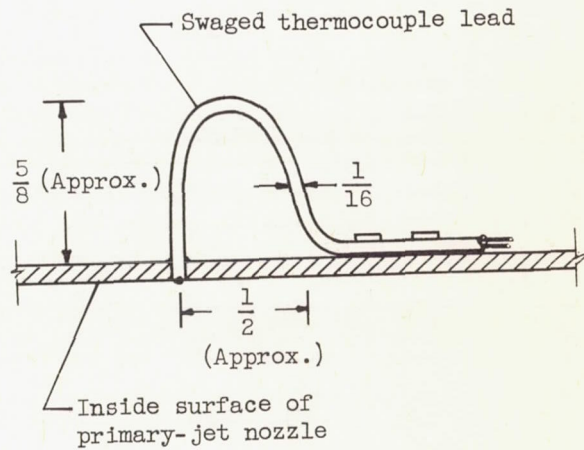


Figure 1. - Sketch of primary-jet-nozzle leaf and filler piece showing thermocouple locations. (All dimensions in inches.)



Side view of typical  
thermocouple installation

CD-5412

Ⓐ Thermocouple

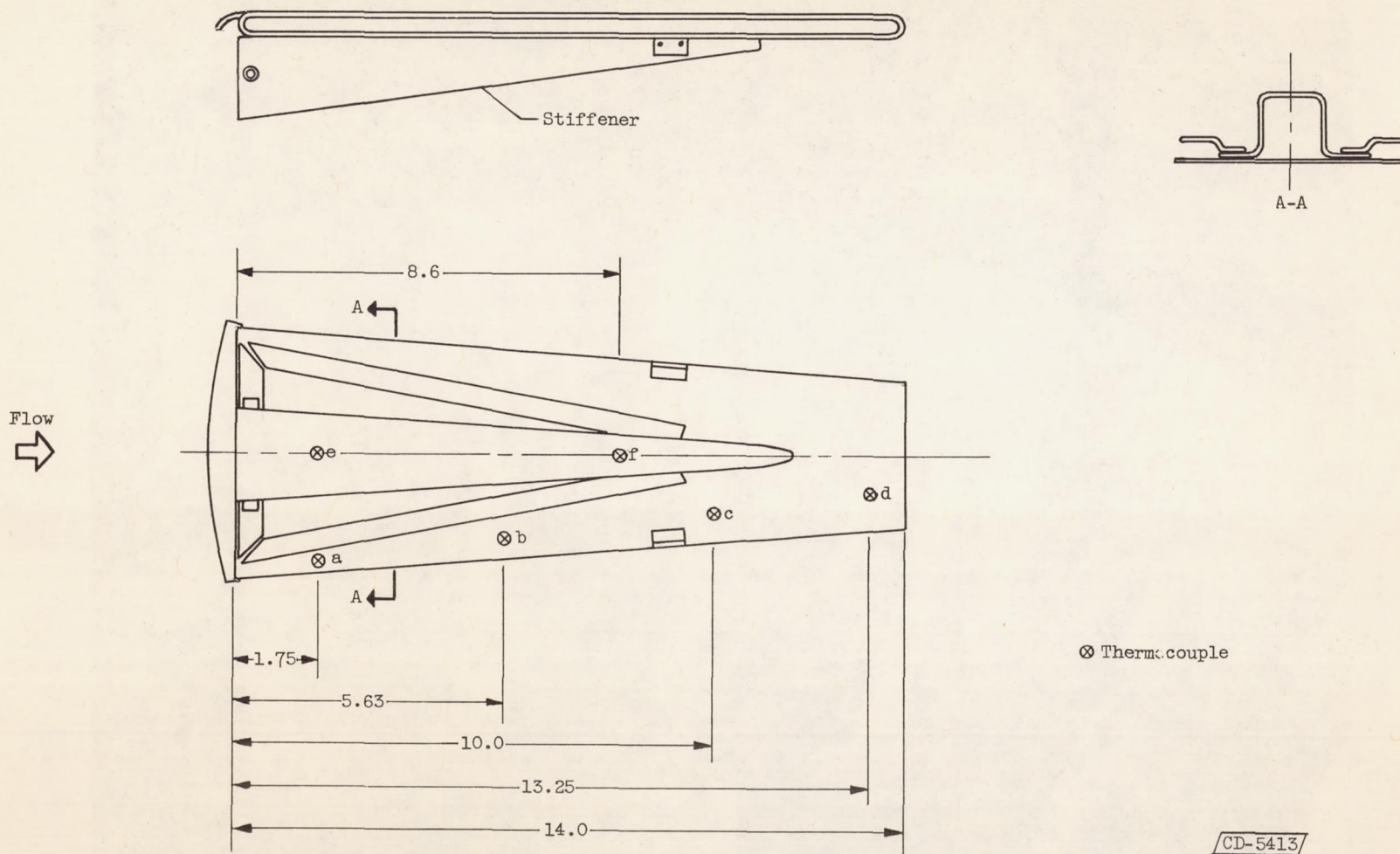


Figure 2. - Shroud leaf showing thermocouple locations. (All dimensions in inches.)

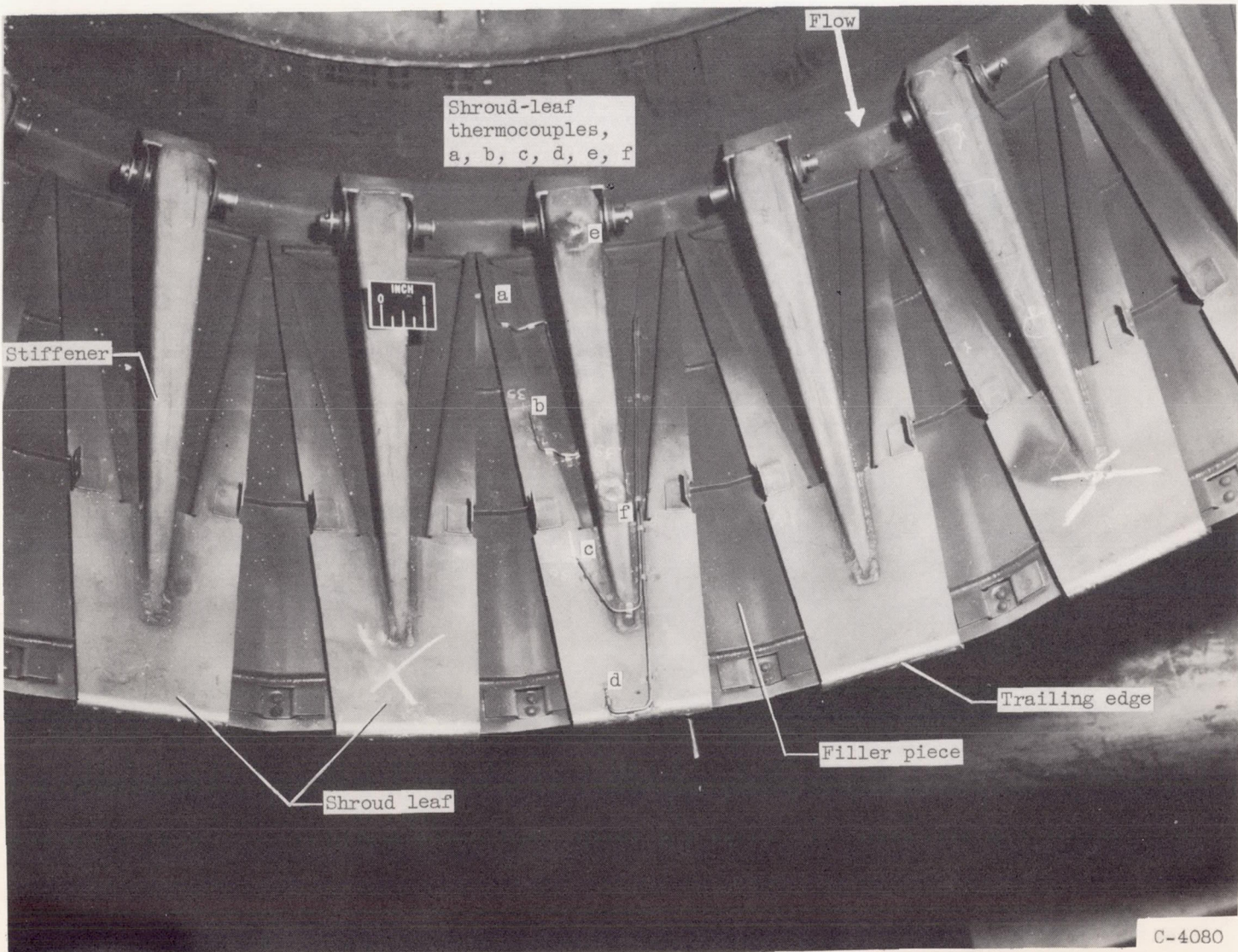
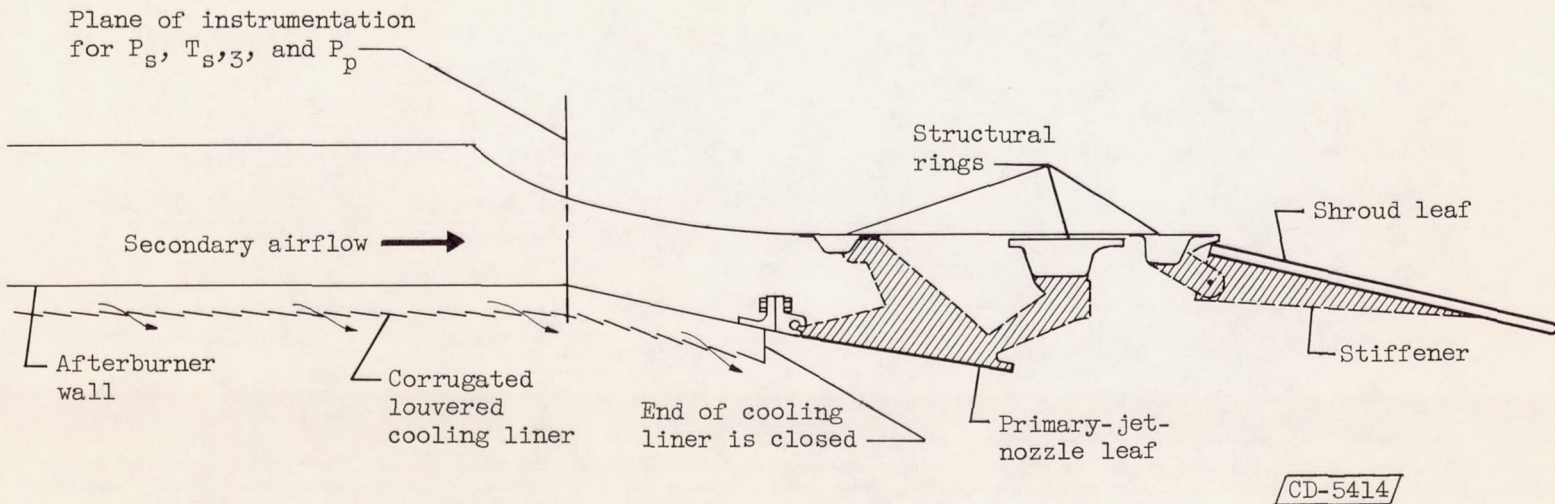


Figure 3. - Inside view of shroud.



CD-5414

Figure 4. - Schematic drawing of iris-type ejector nozzle showing relative positions of primary-jet-nozzle and shroud leaves and regions of secondary airflow passage (shaded areas) partially obstructed by actuating mechanism.

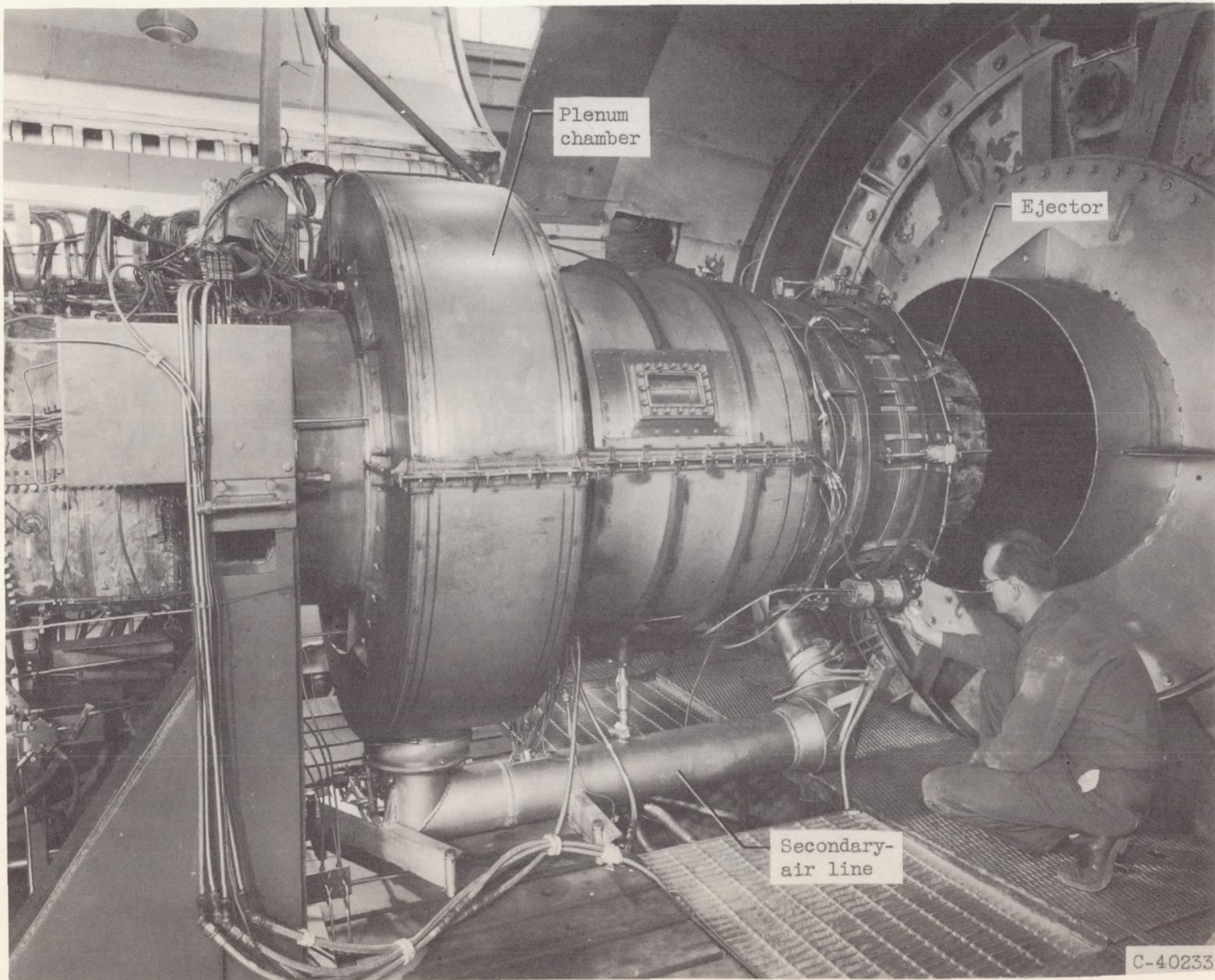


Figure 5. - Exterior view of ejector installation in altitude test chamber.

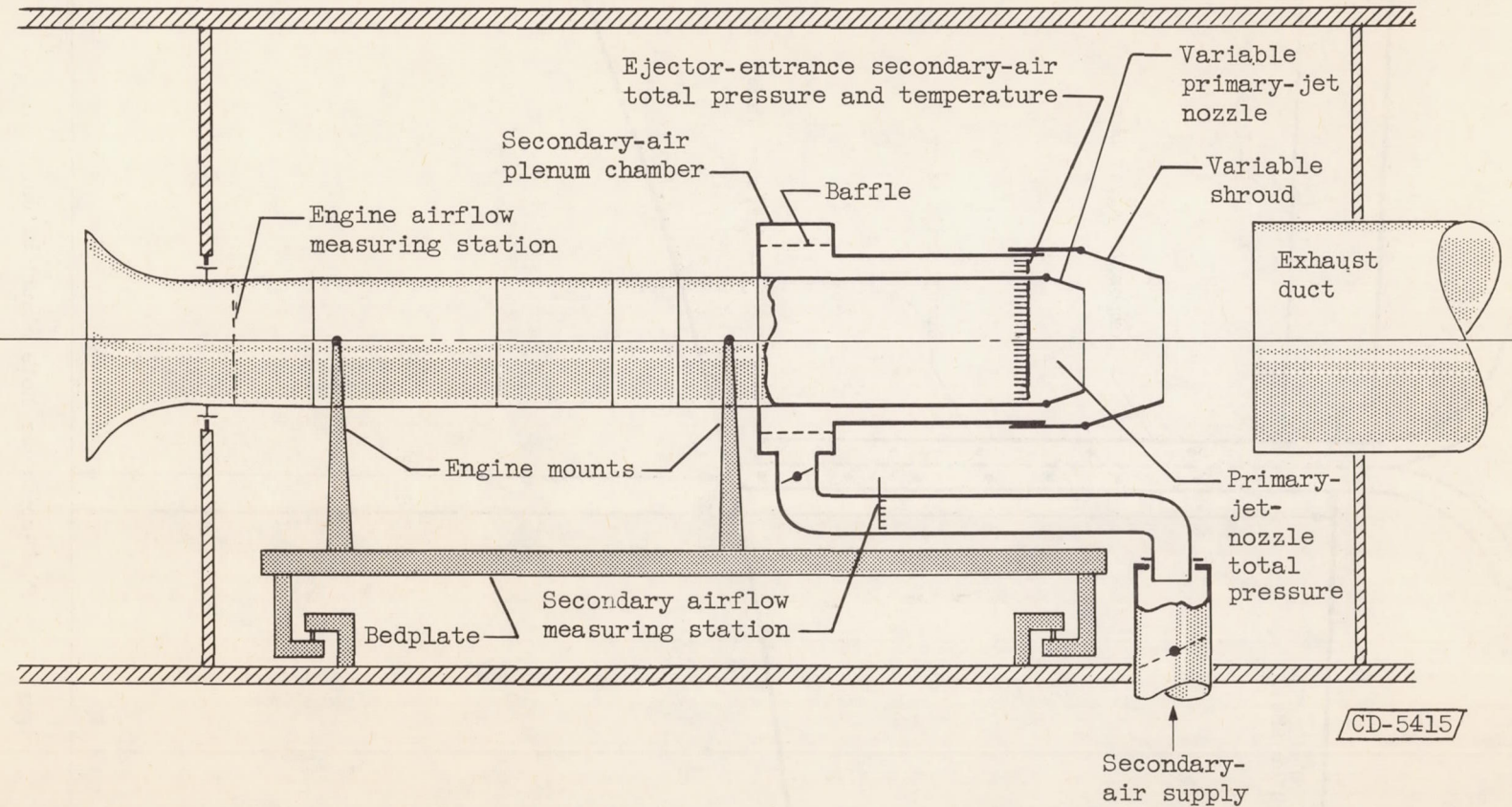


Figure 6. - Schematic drawing of ejector-nozzle installation showing secondary-air ducting.

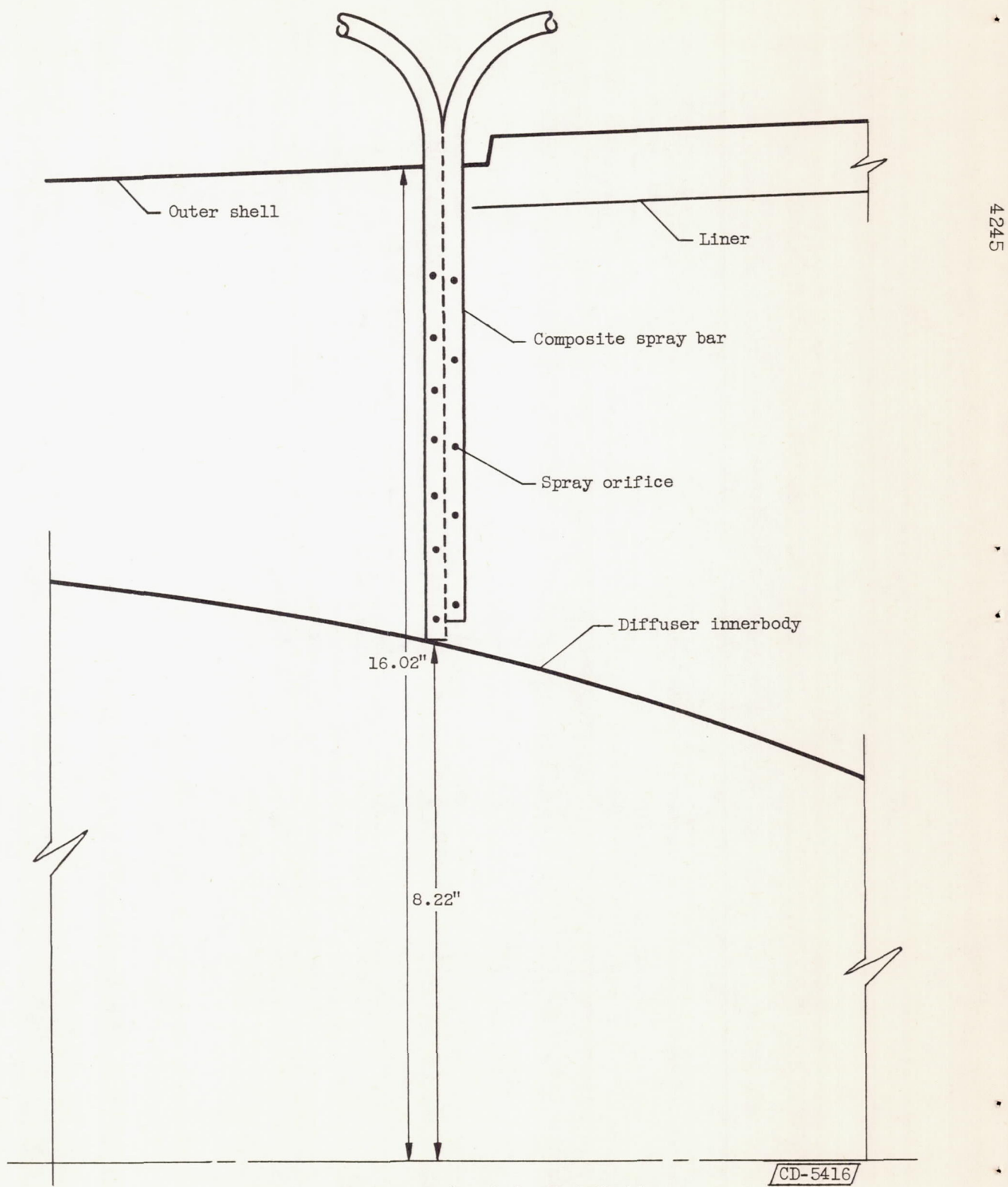


Figure 7. - Fuel-spray-bar hole distribution.

CD-5416

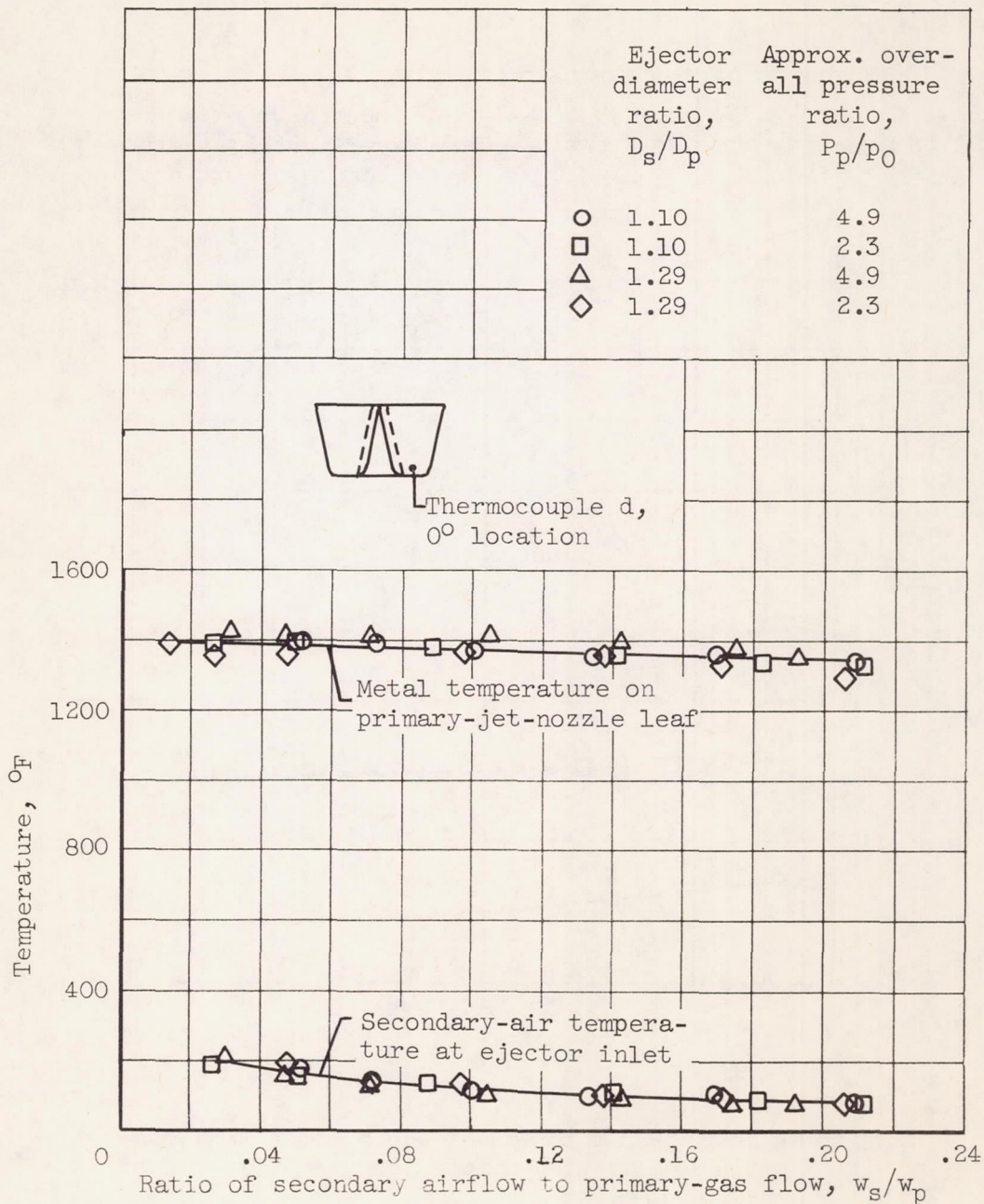


Figure 8. - Temperature of primary-jet-nozzle leaf and secondary air. Primary-gas temperature, approximately  $3450^{\circ}$  R; ejector spacing ratio, 0.725.

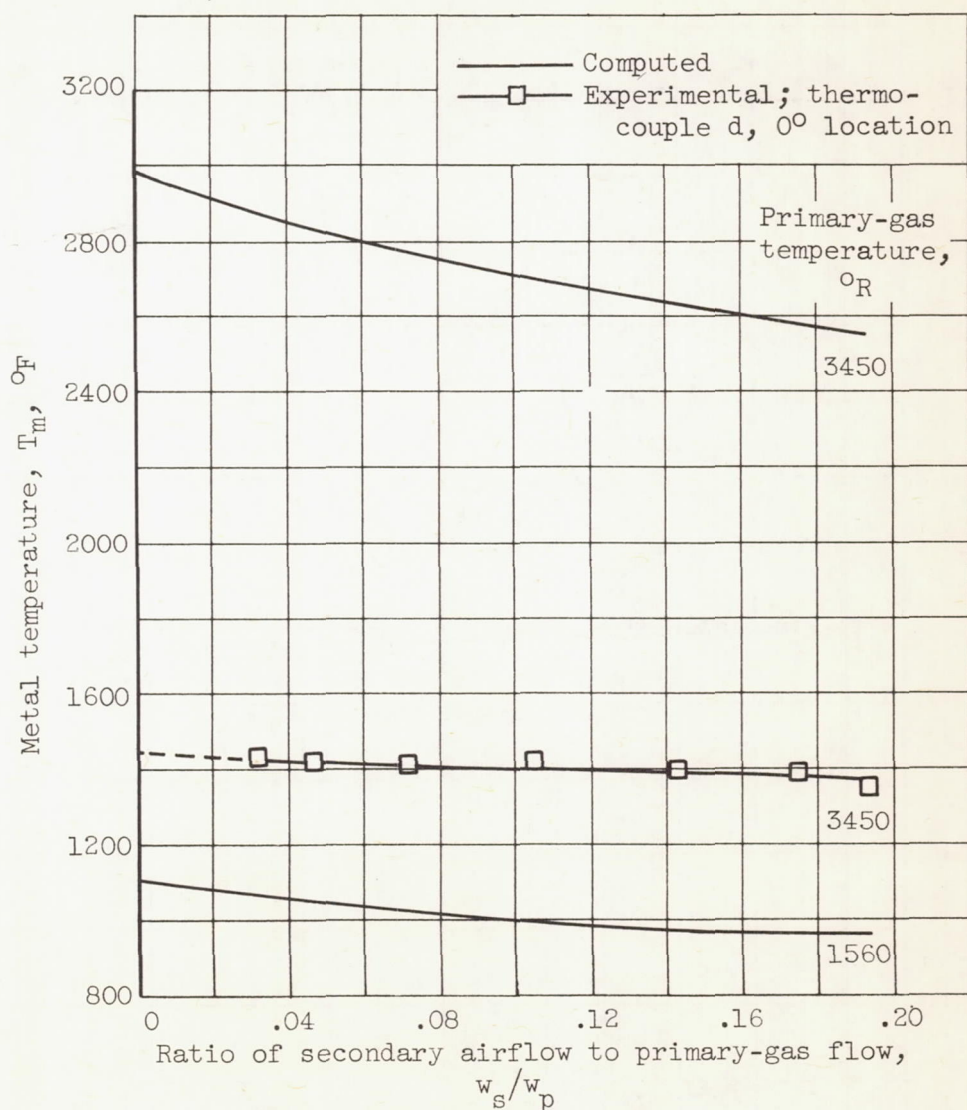


Figure 9. - Comparison of experimental and computed primary-jet-nozzle leaf temperatures at nozzle throat.

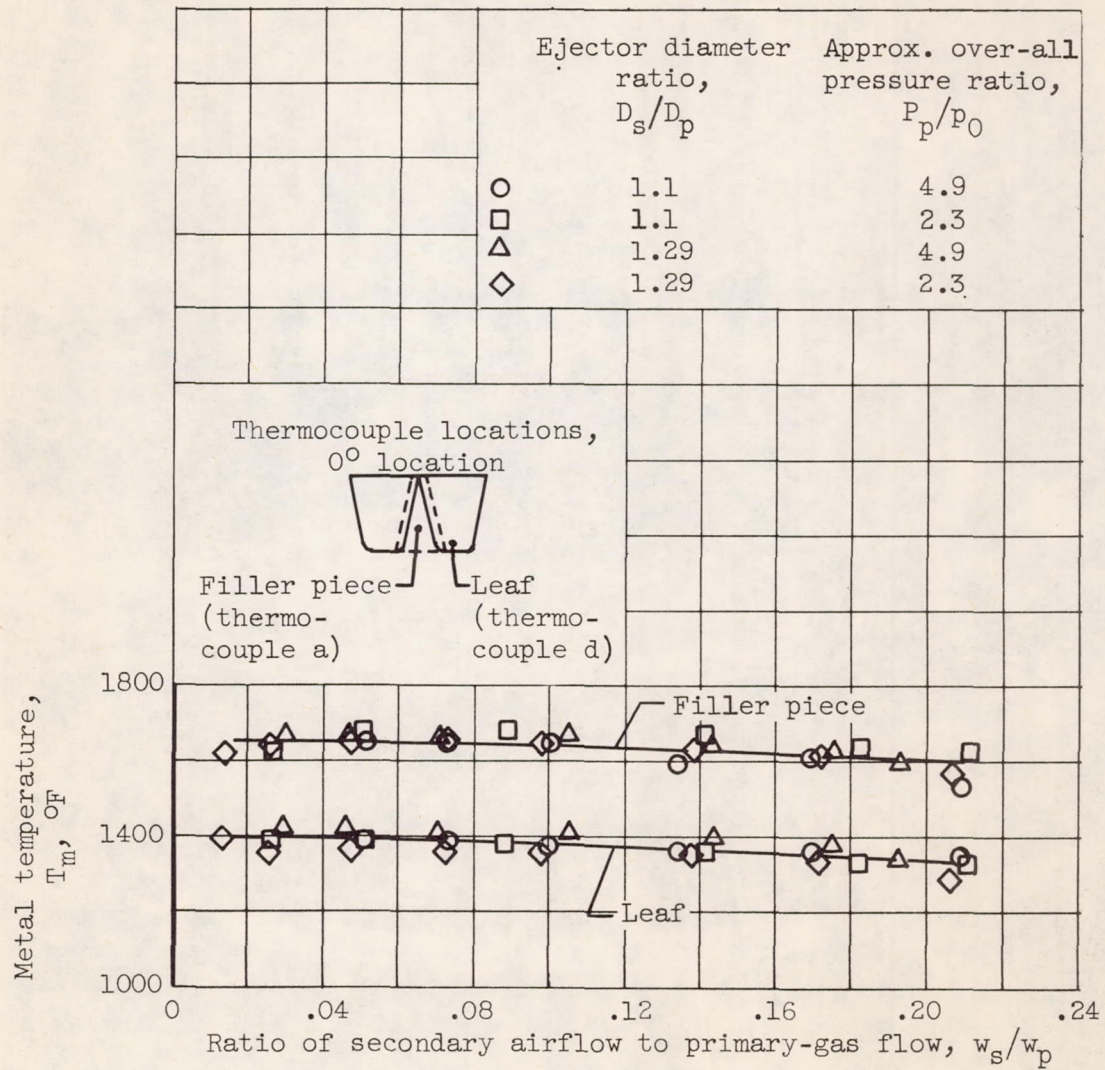


Figure 10. - Comparison of temperatures measured on primary-jet-nozzle leaf and filler piece. Primary-gas temperature, approximately  $3450^\circ R$ ; ejector spacing ratio, 0.725.

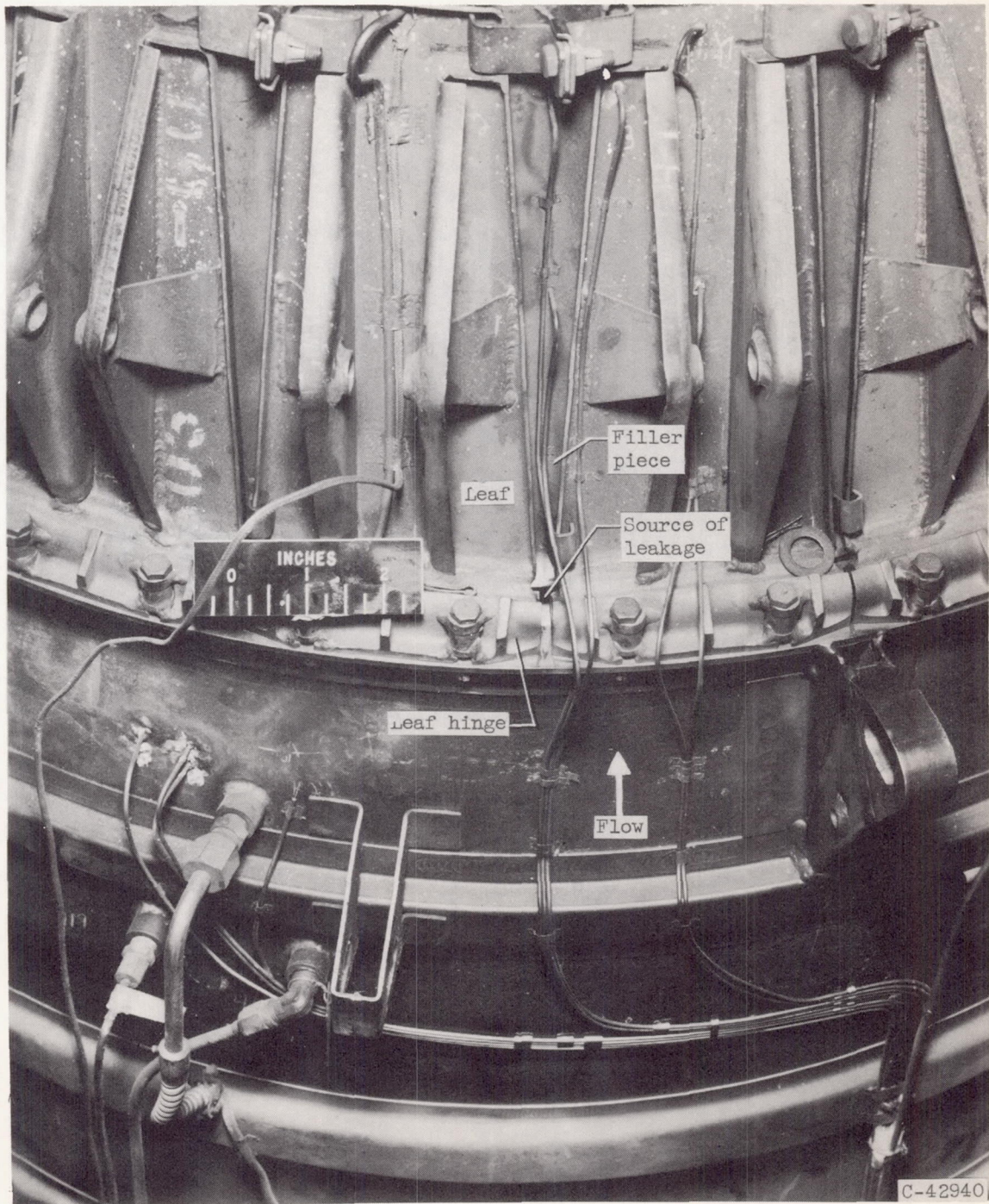


Figure 11. - Primary-jet-nozzle exterior showing source of primary-gas leakage.

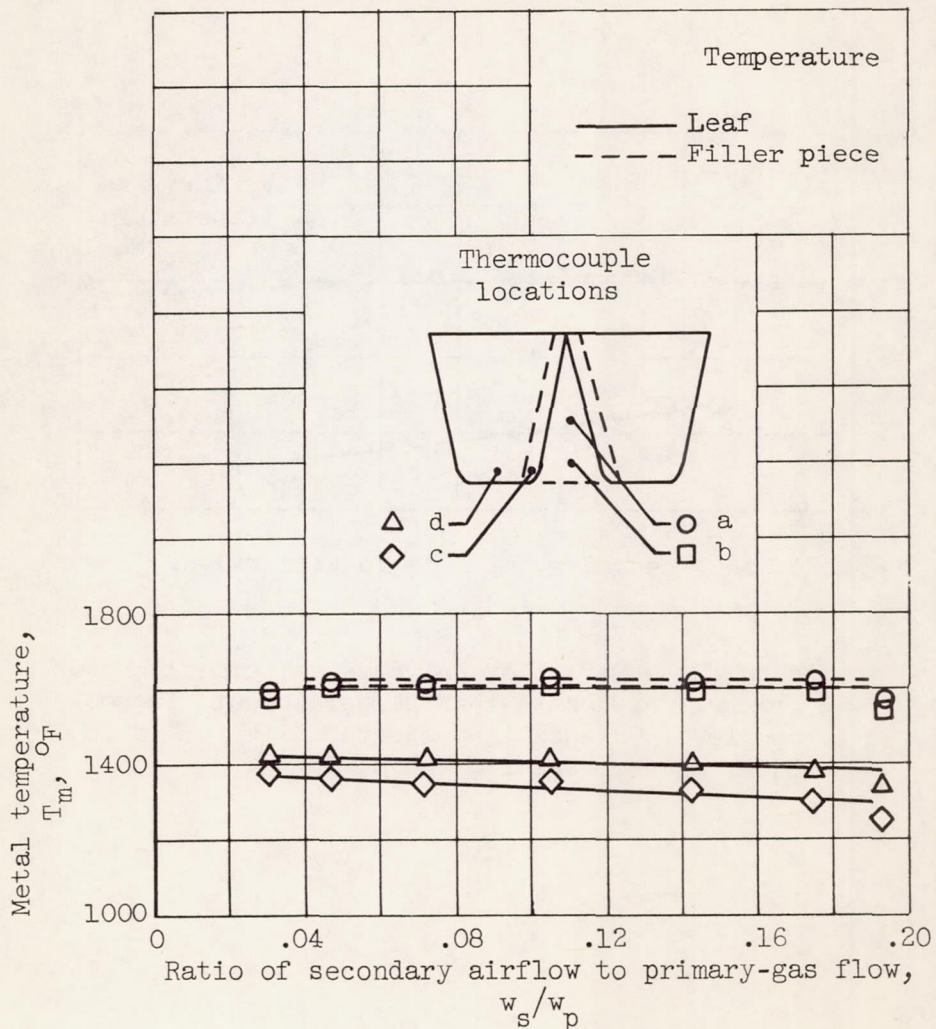


Figure 12. - Comparison of temperatures at various thermocouple locations on primary-jet nozzle.  
Primary-gas temperature, approximately 3450° R;  
ejector diameter ratio, 1.29.

4245

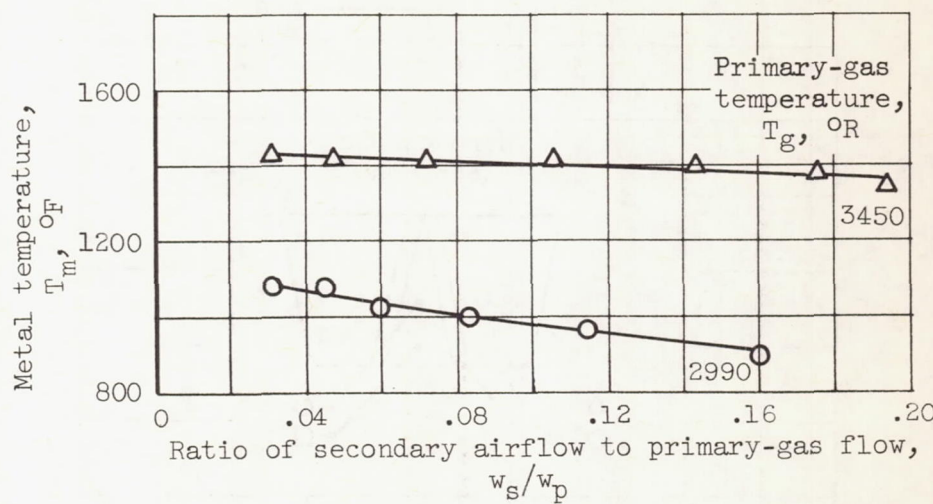


Figure 13. - Effect of primary-gas temperature on primary-jet-nozzle leaf temperatures. Thermo-couple d, 0° location; ejector diameter ratio, 1.29; ejector spacing ratio, 0.725.

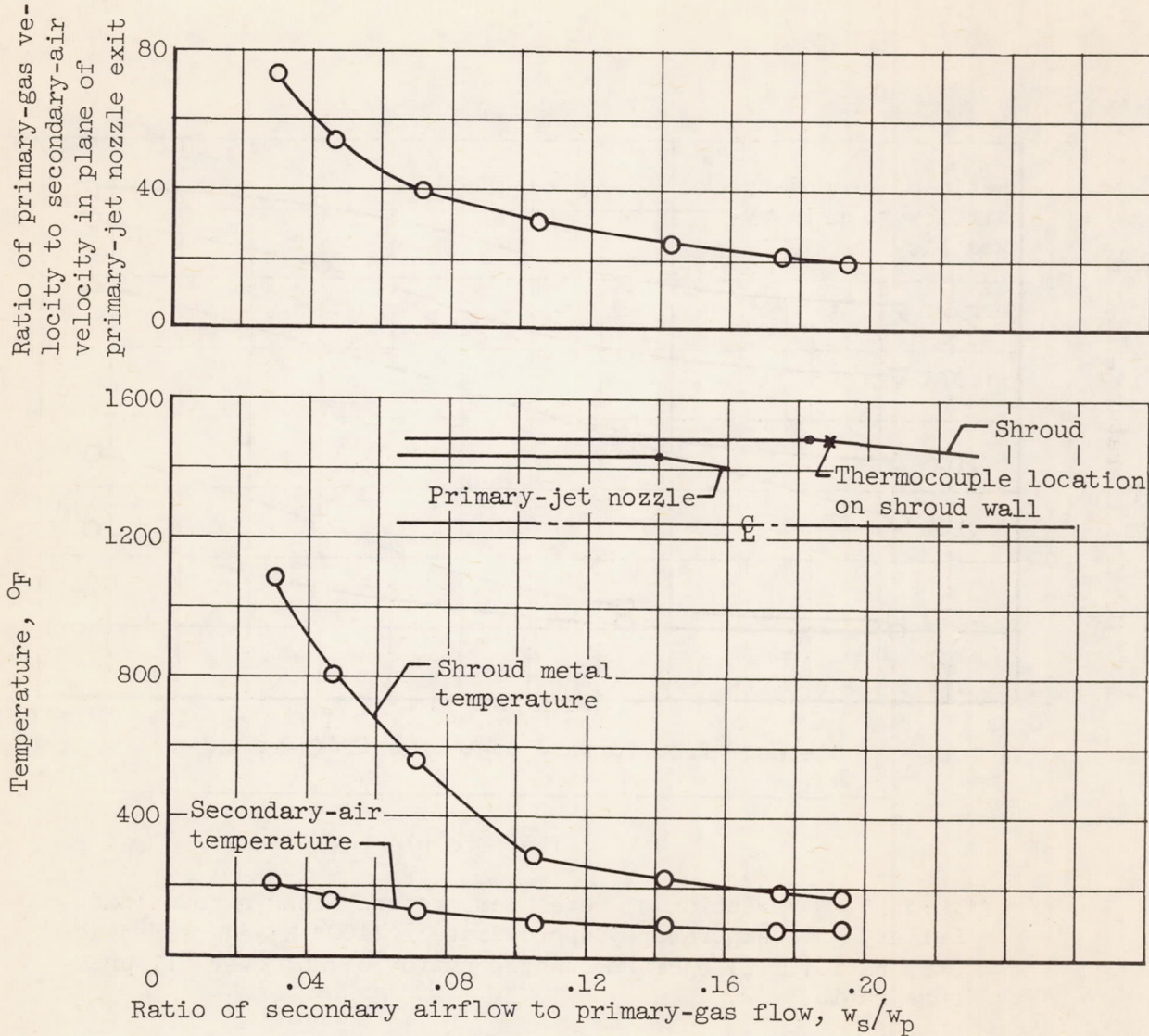


Figure 14. - Effects of mixing of secondary air and primary gas on ejector-shroud heating. Primary-gas temperature,  $3450^{\circ}$  R; ejector diameter ratio, 1.29; over-all pressure ratio, approximately 4.9.

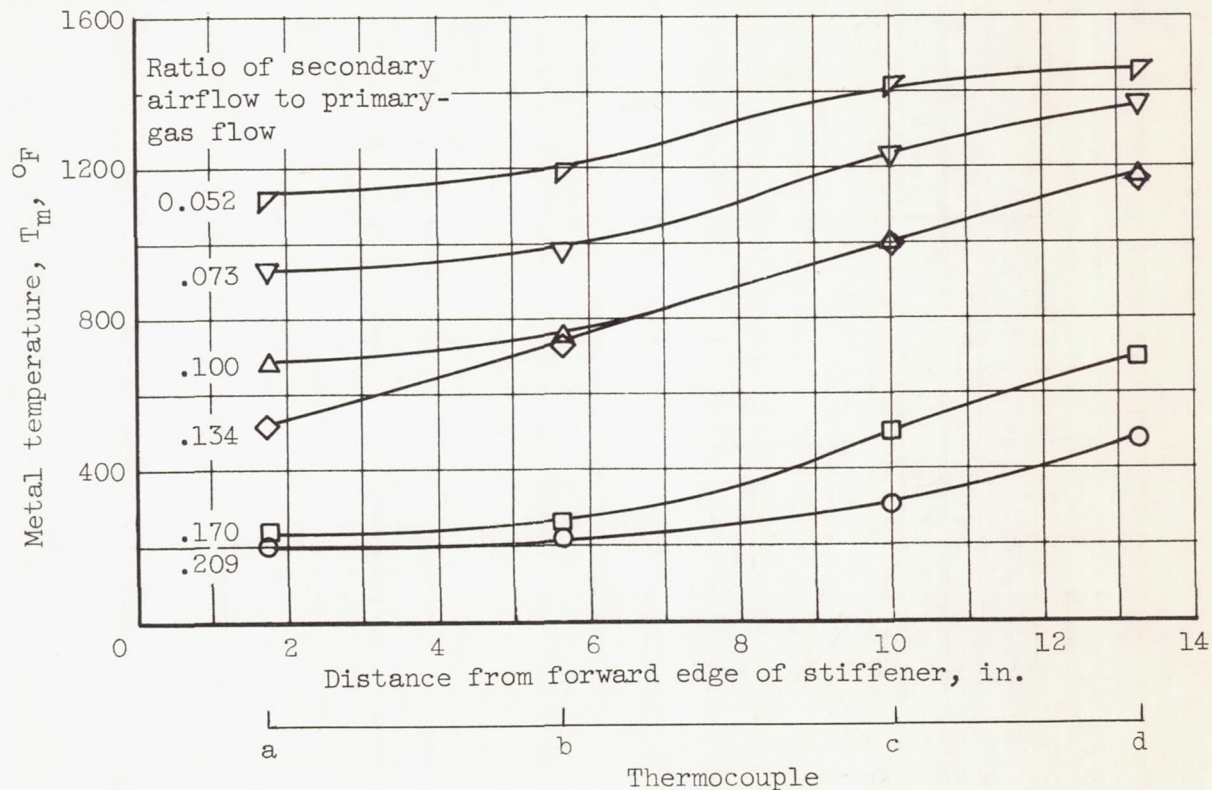


Figure 15. - Variation of metal temperature along shroud leaf.  
 Primary-gas temperature, approximately  $3400^{\circ}$  R; ejector diameter ratio, 1.1; ejector spacing ratio, 0.725; over-all pressure ratio, 4.9.

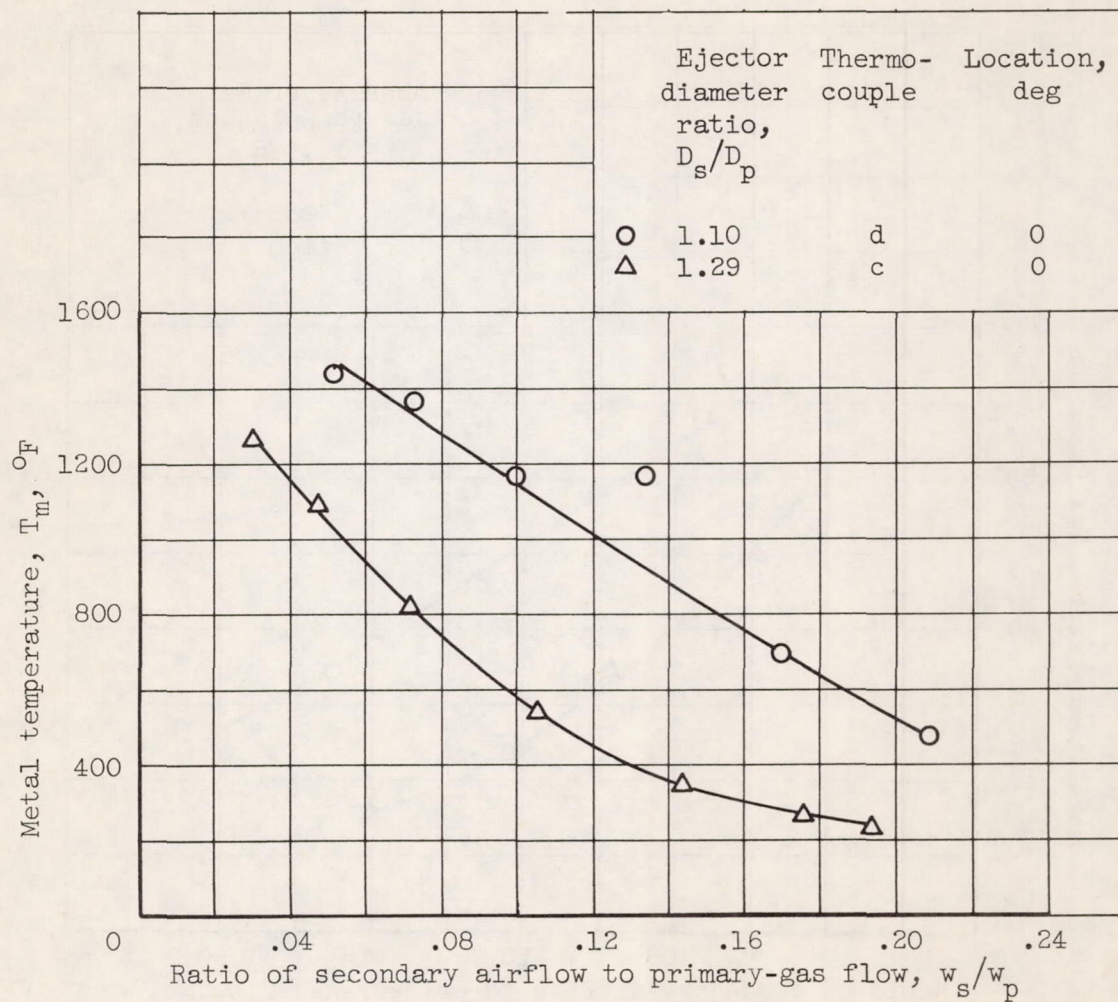


Figure 16. - Effect of ejector diameter ratio on shroud metal temperature. Primary-gas temperature, approximately  $3400^{\circ}$  R; over-all pressure ratio, approximately 4.9.

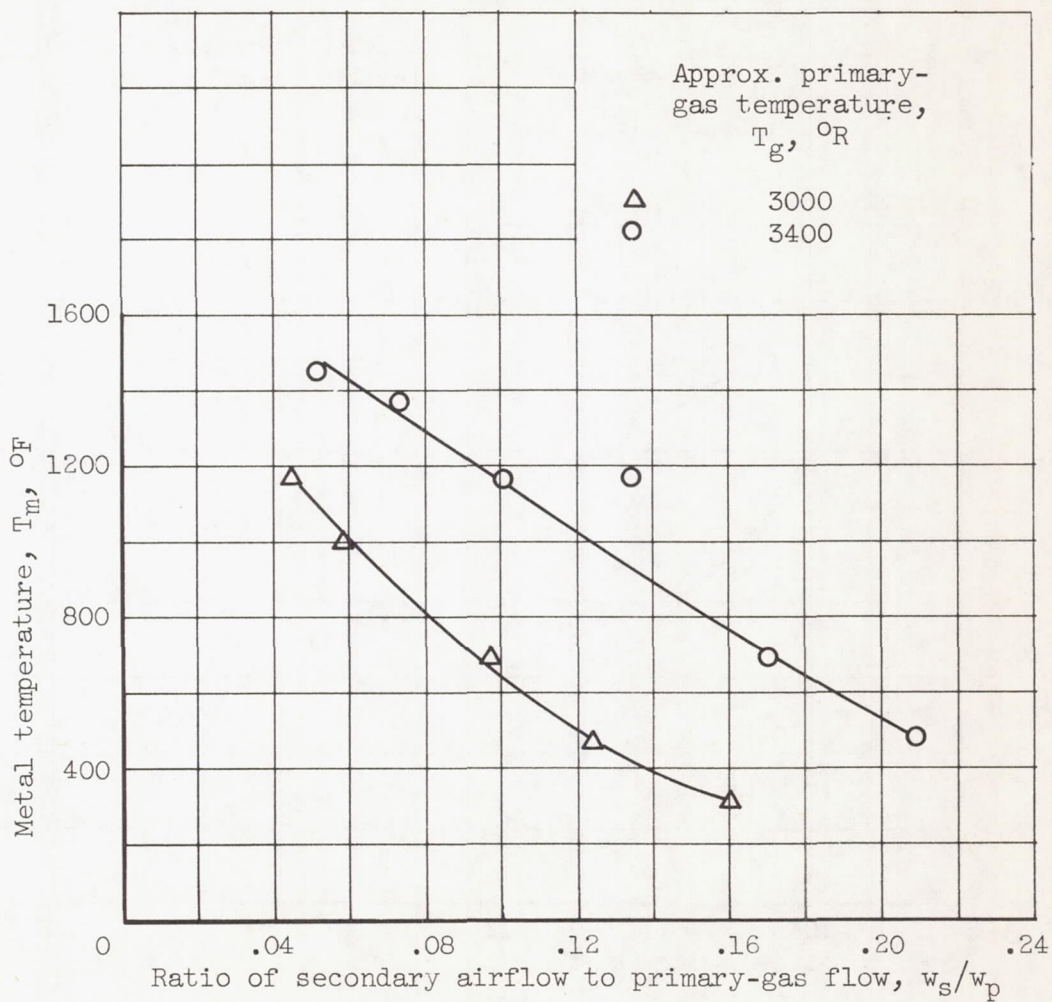


Figure 17. - Effect of primary-gas temperature on shroud leaf temperature. Ejector diameter ratio, 1.10; thermocouple d, 0° location.

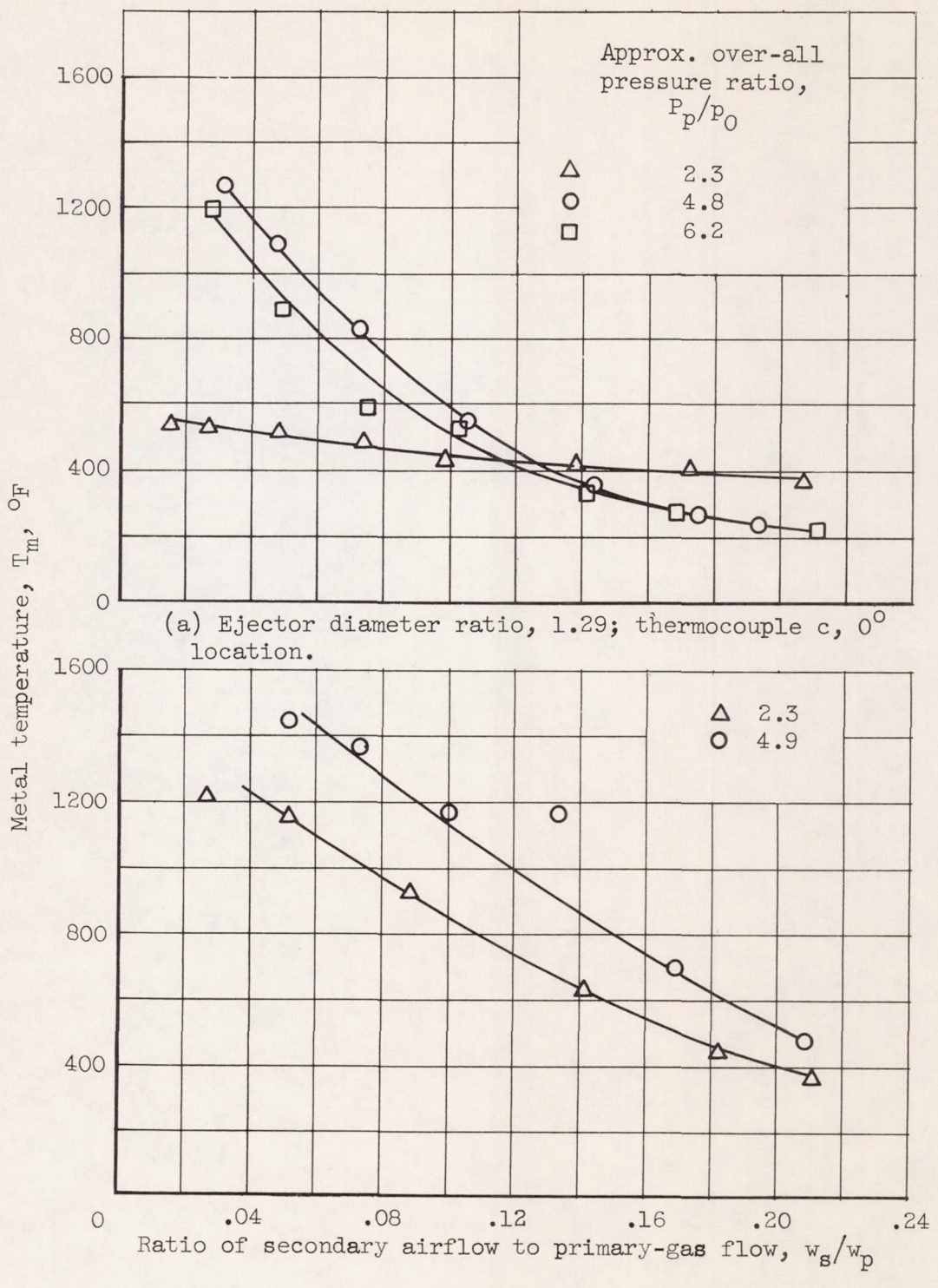


Figure 18. - Effect of over-all pressure ratio on shroud leaf temperature.